ISSUE # 30, 2012

Selenology Today

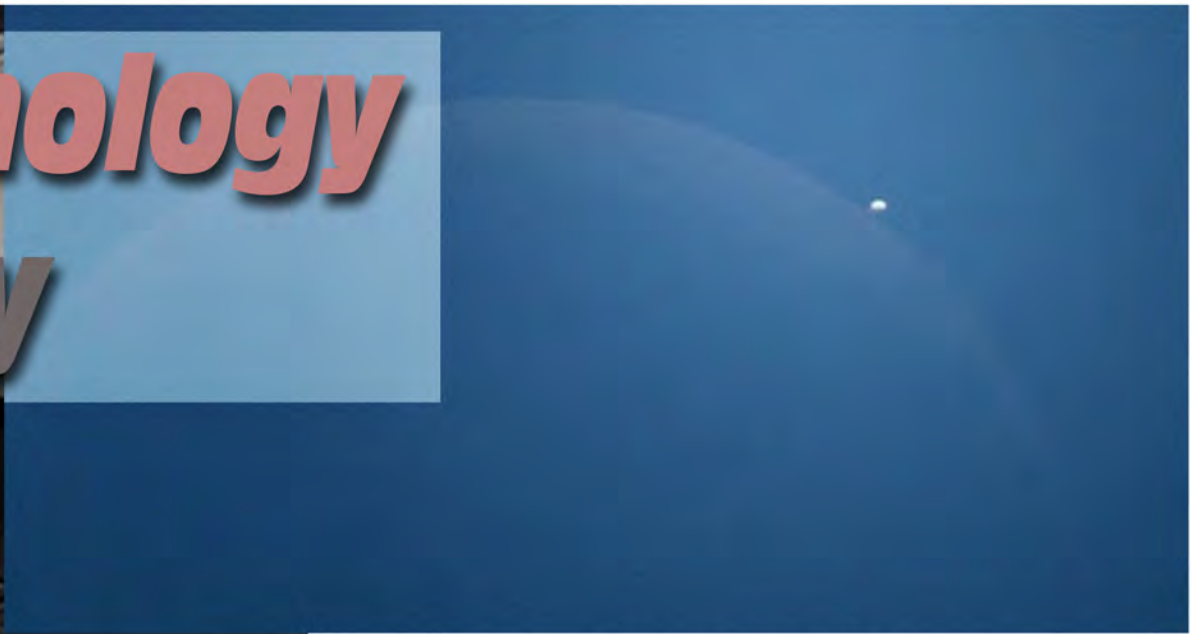

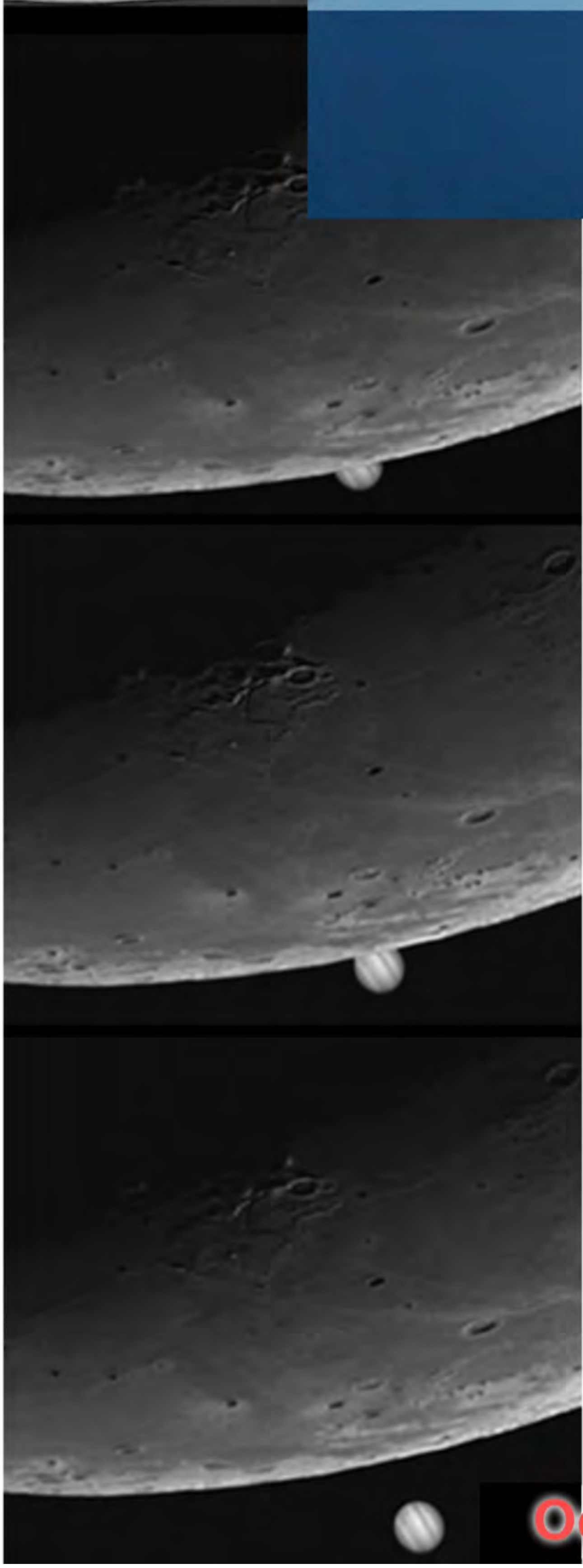

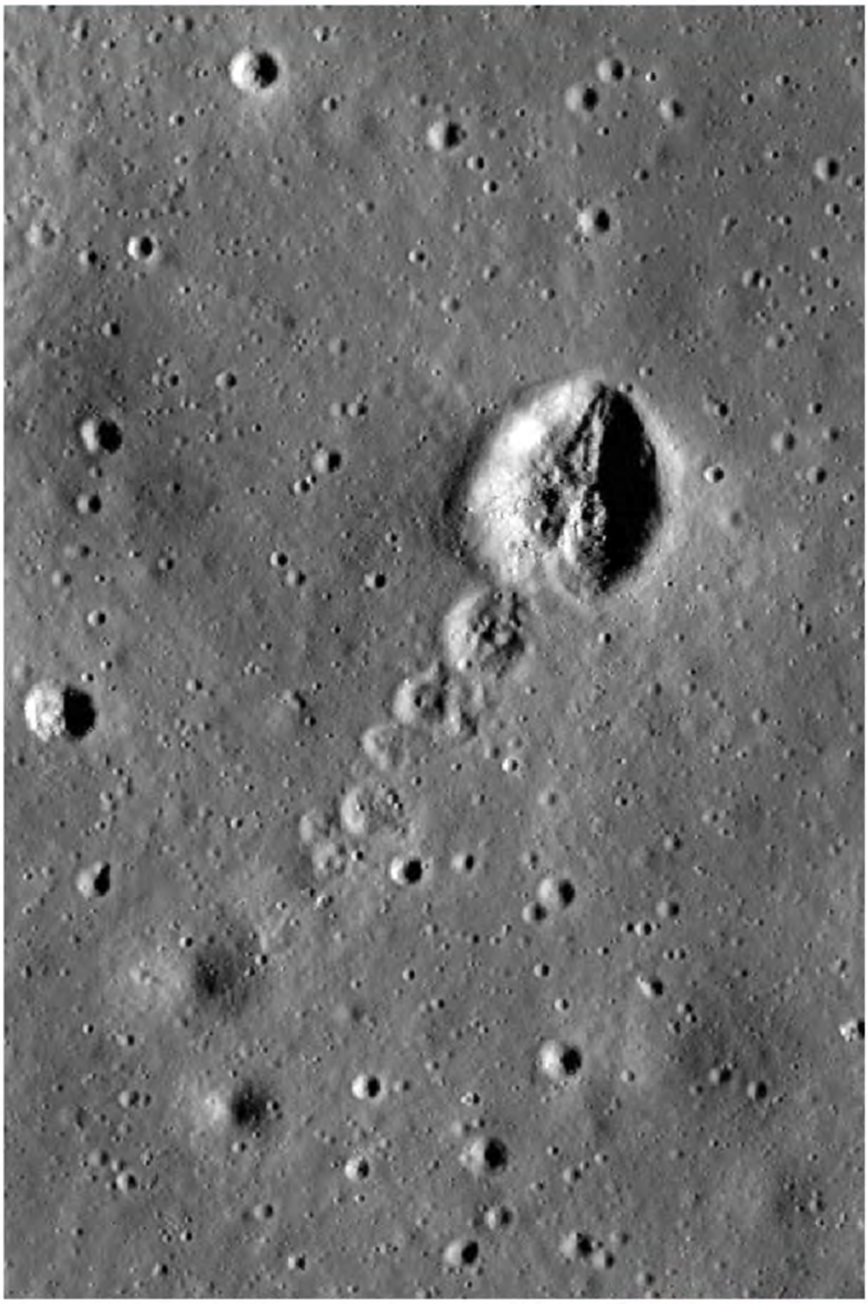

October 2012

Geological Lunar Researches Group

Selenology Today

Selenology Today is devoted to the publication of contributions in the field of lunar studies. Manuscripts reporting the results of new research concerning the astronomy, geology, physics, chemistry and other scientific aspects of Earth's Moon are welcome. Selenology Today publishes papers devoted exclusively to the Moon. Reviews, historical papers and manuscripts describing observing or spacecraft instrumentation are considered.

Selenology Today website

http://digilander.libero.it/glrgroup/

and here you can found all older issues

http://www.lunar-captures.com/SelenologyToday.html

In this issue of Selenology Today not only Moon
(see the contents in following page).

Selenology Today is under a reorganization, so that further comments sent to us will help for the new structure. So please doesn't exit to contact us for any ideas and suggestion about the Journal. Comments and suggestions can be sent to Raffaello Lena editor in chief : gibbidomine@libero.it

Selenology Today

Contents

Zoomorphic Craters 1
Barry Fitz-Gerald

Moretus and the southern lunar region 12
Richard Hill
(Jim Loudon Observatory)

Lunar Kipuka in Opelt 14
Raffaello Lena and Maurizio Morini
GLR group

Lunar Occultation of Jupiter and Venus occurred during July and August 2012 23

COVER
by
Richard Hill (USA)
and
Raffaello Lena (ITALY)
and
LRO from frame M146831612RE

Selenology Today

Zoomorphic Craters

Barry Fitz-Gerald
GLR group

Abstract

Most impact craters appear to be discrete structures, caused by single impactors striking another celestial body to produce an impact crater. This can be taken as the simplest possible scenario, and impact cratering and the form of the astroblemes produced are subject to many complicating factors such as impact angle and target or impactor strength and composition. Observation suggests that many Earth Crossing Asteroids (ECA's) appear to be composed of loose aggregations of material (rubble piles) and as such their effects may more resemble the 'scattergun' effect of a shotgun rather a rifle bullet when impacting another body. The amount to which such bodies are prone to tidal disruption in the Earth – Moon space is open to debate, but it would appear possible that such a process can lead to the formation of crater chains as the individual fragments of the original body or 'progenitor' (Bottke, et.al, 1997) become separated along their trajectory in the manner observed for Comet Shoemaker-Levy 9. Prominent lunar crater chains such as the 'Davy Chain' are generally accepted that these are the result of such tidally disrupted impactors, this article explores suspected crater chains at a much smaller scale, and differing morphology.

High resolution lunar images from the Lunar Recognisances Orbiter mission have enabled a growing body of Citizen Scientists to explore fine detail of the lunar surface, most notably via the Moon Zoo project. One feature identified by a participant of that project in 2010 is known as 'Caro's Tadpole' (Fig.1), a small, anomalous impact crater chain, vaguely reminiscent of a larval frog, hence the nickname.

The 'head' of the tadpole consists of a shallow, elongate crater, approximately 130 meters along its major axis, with the 'tail' of the tadpole being made up of a series of small, partially overlapping, shallow craters, extending in a line to the south-west.

Whilst the 'tadpole' is formed by a 'chain of craters', it is not a typical 'crater chain' such as the 'Davy Chain' or the crater chain in Mendeleev, features believed to have originated from the impact of a string of debris formed by a tidally disrupted impactor. By adjusting the contrast on one of the LRO frames as shown in Fig.1B, the extent of the ejecta blanket is revealed, showing

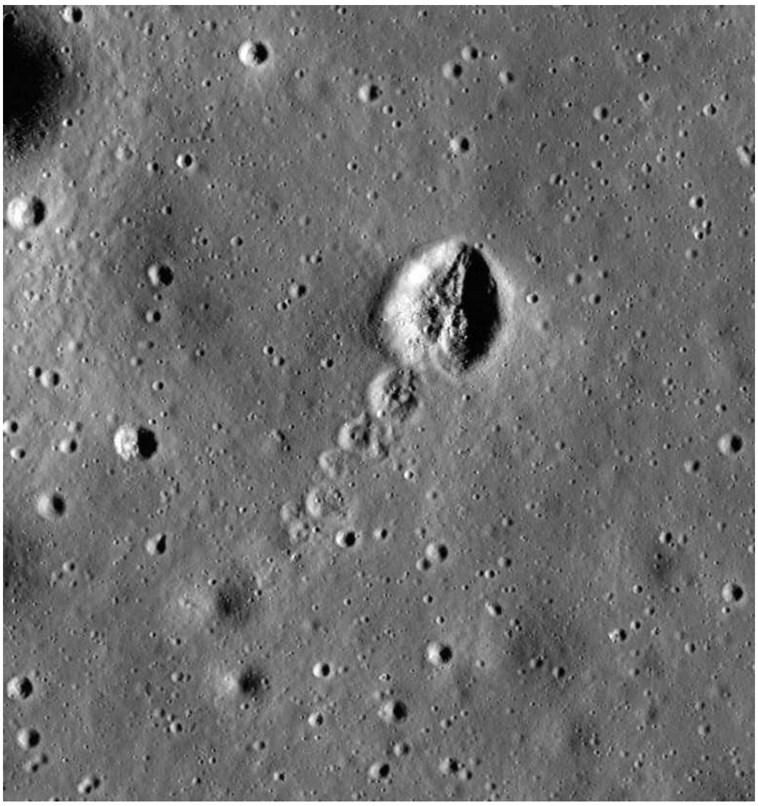

Fig.1A 'Caro's Tadpole' from LRO from frame M146831612RE.

Selenology Today

that the 'head' and 'tail' of the tadpole share a common ejecta blanket, indicating an origin in the same impact event. There is a clear Zone of Avoidance to the north of the main crater, suggesting that this is the up-range direction and that the crater chain extends towards the down-range direction. A possible interpretation of the structure therefore is an oblique impact from the north-east (top-right of the image) to form the main crater, with either target or impactor material being ejected downrange to form the chain of craters. Alternatively the chain of craters may have formed from the simultaneous but separate impacts of debris travelling with the main impactor following earlier disruption of a small 'rubble pile' type body.

Fig.1B 'Caro's Tadpole' from LRO from frame M106726943RE (B). The frame has been contrast enhanced.

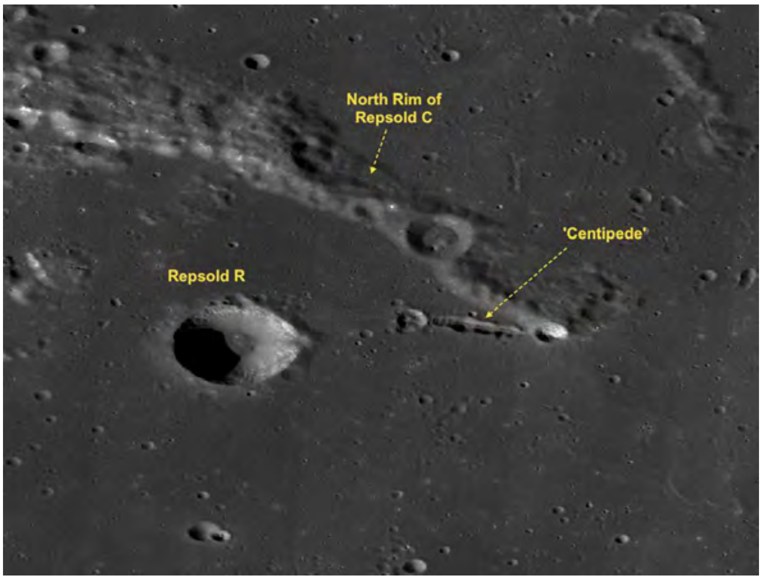

Fig.2 Location of the 'Centipede' crater chain.

Using another zoomorphic name as a device to identify the structure under discussion, the following article describes an unusual crater chain located within the battered northern walls of Repsold C (Fig.2). This structure is approximately 25kms long and is orientated in an approximate east – west direction. It can be sub-divided into three separate units running from east to west, with narrow gaps between each unit. The structure will be referred to as the 'Centipede' for reasons that will become apparent later in this article.

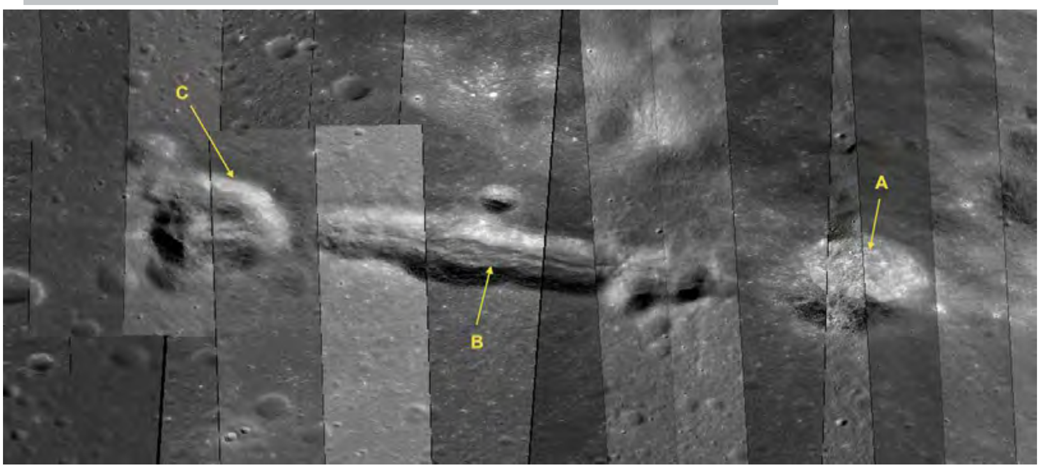

Fig.3

LRO image of 'Centipede' crater chain, showing crater A truncating the promontory slope, elongate crater B with central ridge and terminal crater C.

Fig.3 is a Lunar Reconnaissance Orbiter (LRO) image of the 'Centipede' showing the location of the various sub-units to be discussed. The easternmost component is an impact crater A, located at the base of a promontory formed by the eroded northern rim of Repsold C, near its southern termination beneath the basalt plains of Oceanus Procellarum.

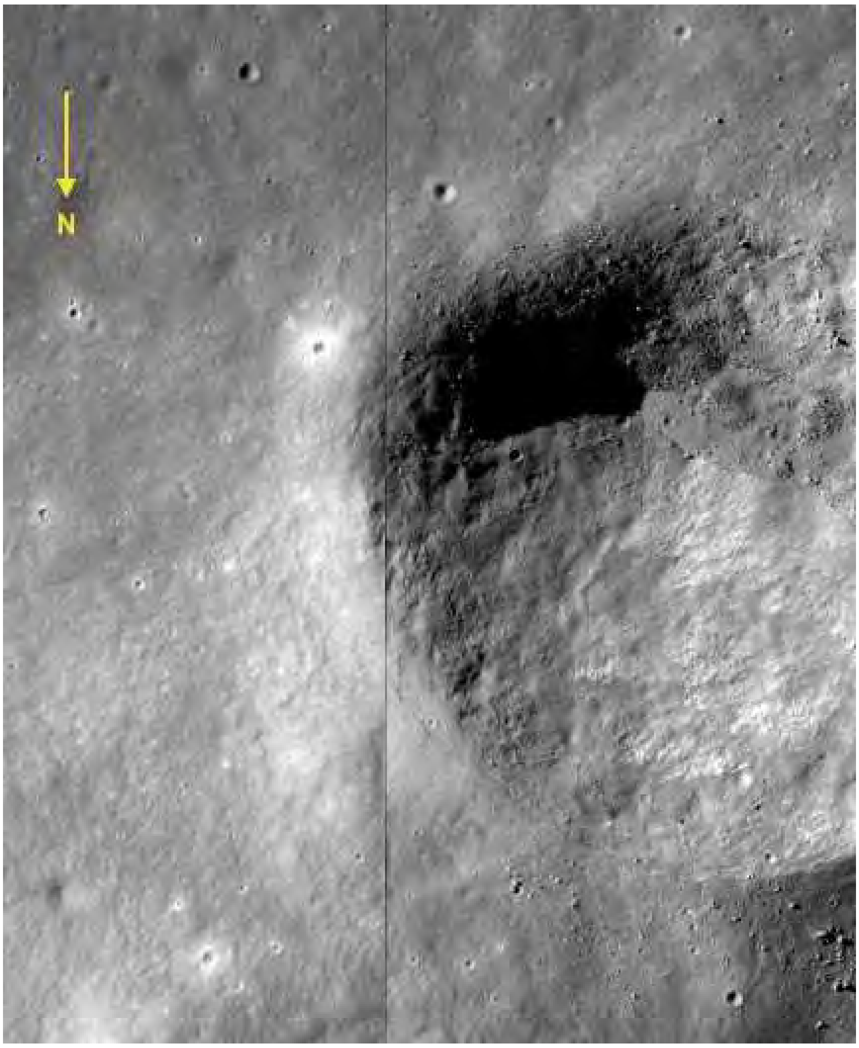

Geological Lunar Researches Group

Fig.4 LRO Detail of Crater A showing steep northern wall and melt pool on floor. Note texture of northern inner wall indicating mass wastage.

Fig.5
LRO Topographic profile of crater A from north (left) to south (right) showing steep slope of northern wall and location of crater at the base of

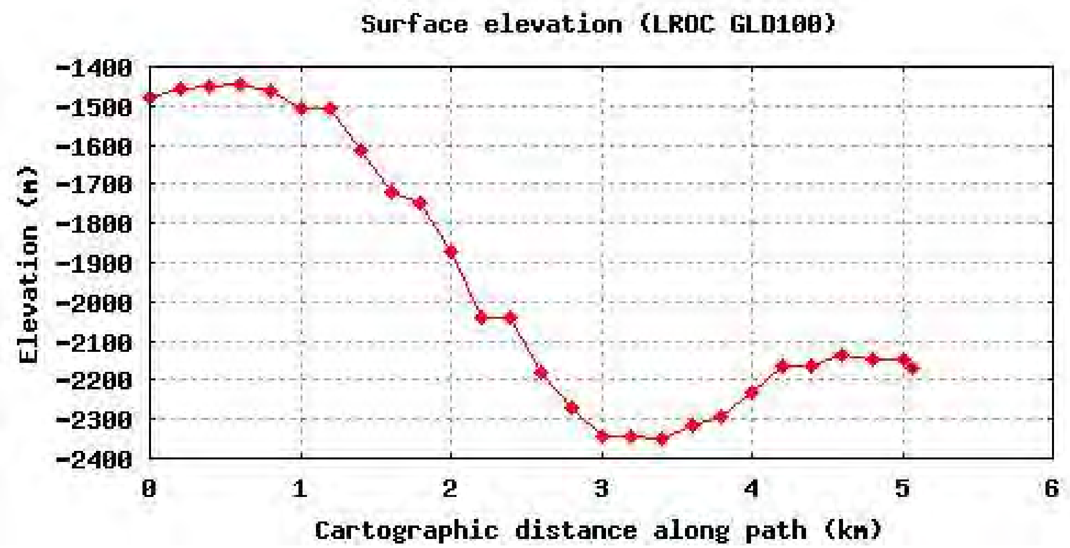

With an approximate length of 2.5kms along the east-west axis, crater A appears recent in lunar terms, with rubble strewn walls and a smooth impact melt pool on it's floor. The outline of the crater is modified by it's location at the base of the promontory to the north. It is possible that the impact sheared off the end of this promontory, resulting in the steep slope forming the craters' northern inner wall. This slope, as can be seen from Fig.4 and the Topographic profile in Fig.5, is probably sufficiently steep to be subject of constant mass wastage, and the northern part of the crater floor is therefore probably obscured by loose debris.

Selenology Today

To the west of A, and separated by what appears to be a short gap, is an irregularly elongate crater B of variable width, with a conspicuous central ridge apparently running along it's 14 km length. The LRO images (Fig.6) shows that this crater varies in nature along the course of it's length from east to west. The central ridge can be traced along the length of the crater, appearing at it's widest at the point where B is at it's widest, and adjacent to a fresh impact crater just north of the northern rim. This observation would suggest that the ridge is the result of mass wastage from the northern and southern walls of B with the accumulation of the debris along the elongate crater floor. The southern rim of B in particular appears particularly 'scalloped' again indicative of slope failure along this edge.

The depth of B can be gauged by reference to Fig.7 which indicates a difference in height of some 300 meters between the rim and the crater floor approximately mid way along it's length. This depth profile is not continued into the westernmost part of B, which is only 100 meters deep as shown in Fig. 8, whilst the topography appears more 'subdued' than that to the east. The central ridge can still be seen here, but is far less conspicuous that throughout the remainder of the length of B. The LRO image (Fig.6) hints at the existence of transverse ridges across B, at various points along it's length, but these are subtle and not apparently significant features.

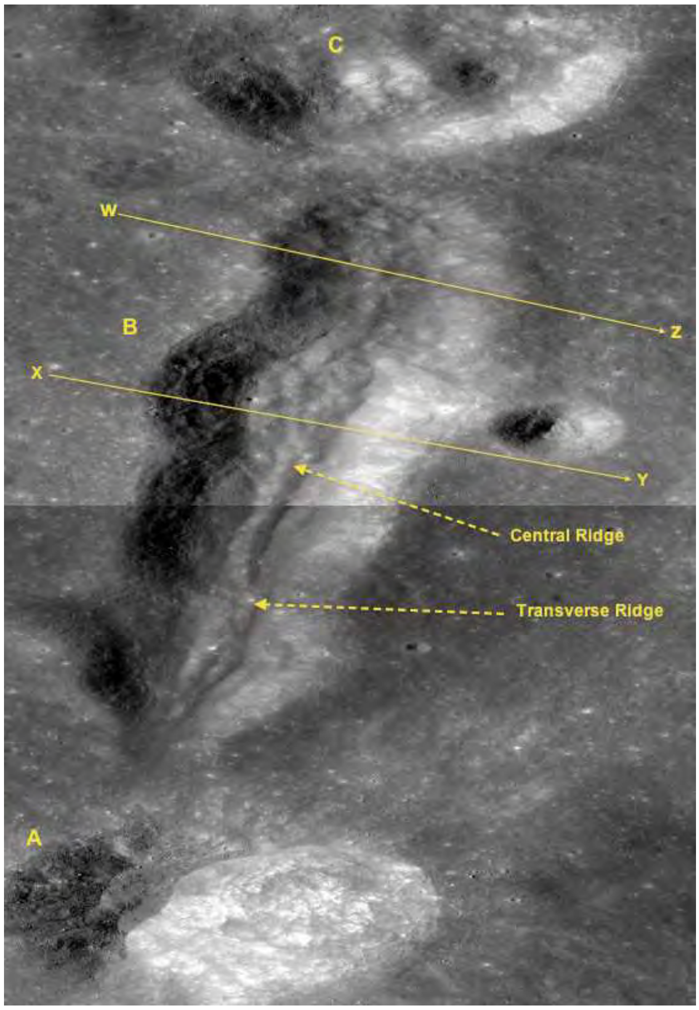

Fig.6
A view of the 'Centipede' looking from it's eastern end showing craters A, B and C. LRO frames M186363791LE and M186363791RE
(North is to the right).

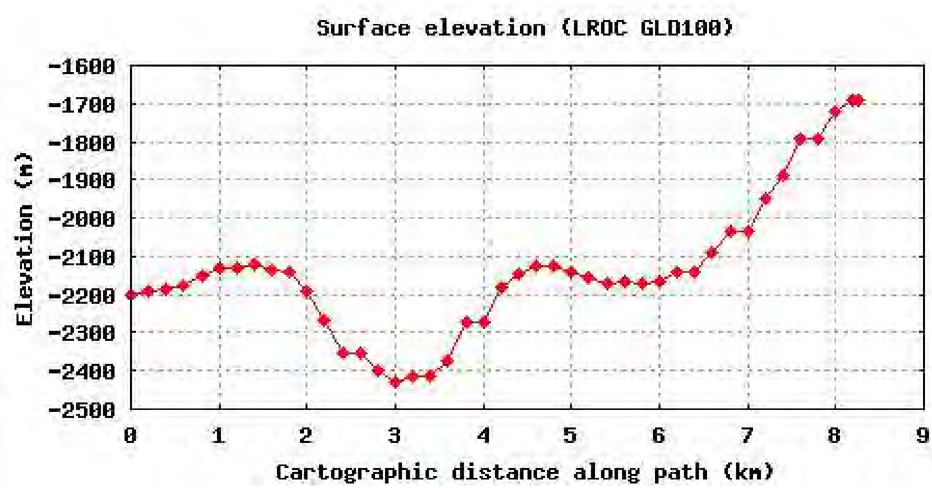

Fig.7 LRO Topographic profile along line X – Y in Fig.6.

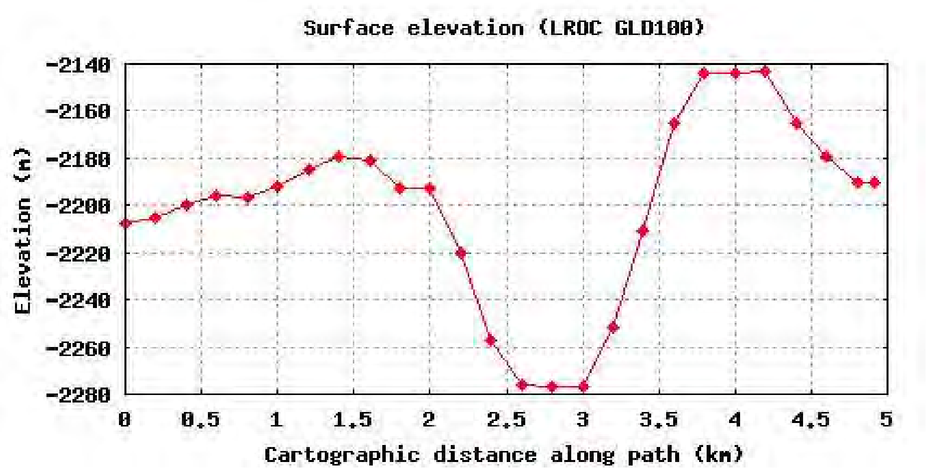

Fig.8 LRO Topographic profile along line W – Z in Fig.6.

The Lunar Orbiter image of the area, Fig.9 shows B in a completely different light, no pun intended, with the impression being that of a chain of four or more irregular shallow craters with, in places distinct intervening septa, rather than a continuous uninterrupted trough.

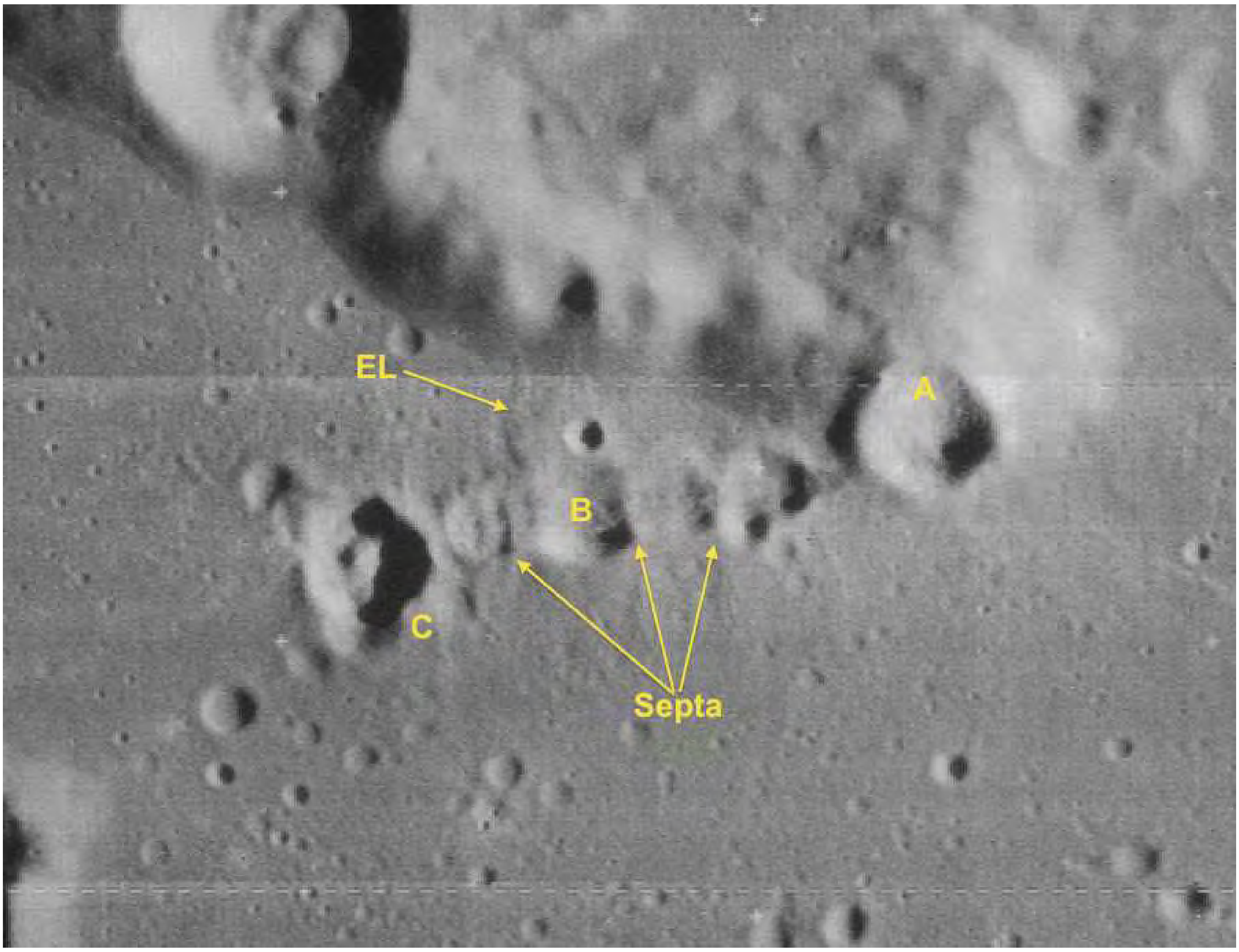

Fig.9 Detail of Lunar Orbiter frame LO-IV-189-H3. EL=Ejecta Lobe

Selenology Today

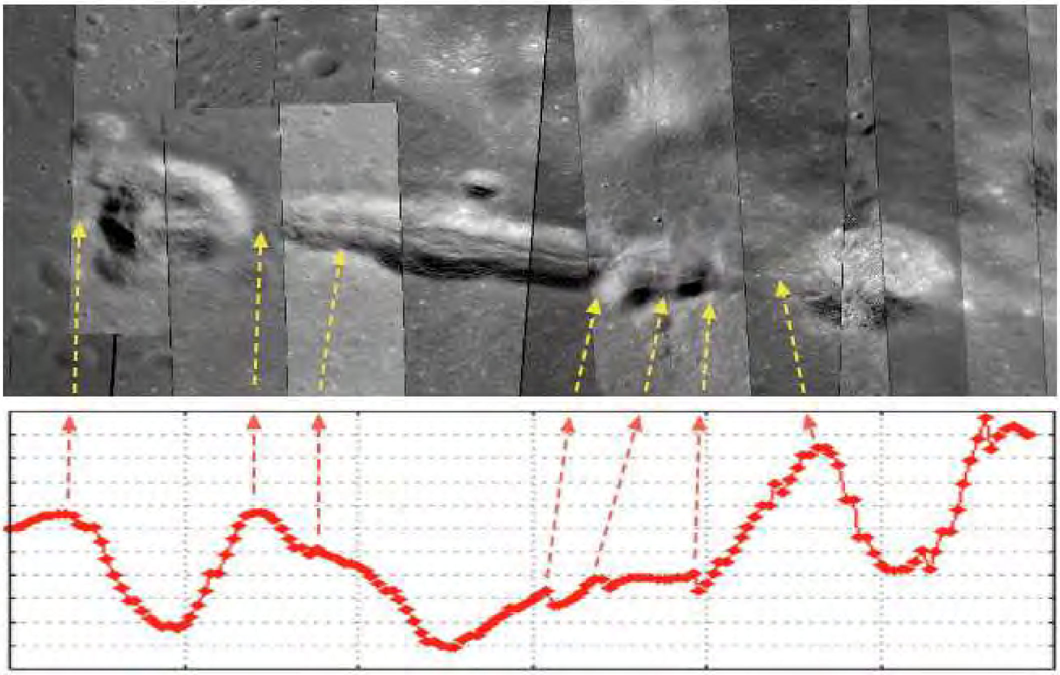

Fig.10
LRO Topographic profile along the length of the 'Centipede' showing the locations of transverse septa.

This image serves to emphasis the way B appears to be crossed by a number of transverse septa, not immediately apparent in the LRO images themselves. The LRO Topographic profile tool however renders these transverse features visible (Fig.10) suggesting that the Lunar Orbiter frame in many ways presents us with a more informative image that it's modern counterpart.
At the western end of this structure, crater C forms the head of the 'Centipede' and shows the rather irregular floor hinted at in Fig.11. Another apparent gap separates B from C. The crater appears to have an irregular ridge like structure on it's floor which is in line with the central ridge of B, whilst to the north-west and south-west it appears to overly 'older' craters that give C the appearance of having 'ears' on either side. The central ridge is readily visible in the LRO image in Fig.11, but the accompanying profile reveals that it's topography is subtle, and does little to reduce the smooth crater profile and depth of some 300 meters. This figure of 300 meters appears to be the overall depth of all the features discussed so far, with the exception of the western portion of B which is much shallower. The apparent older craters forming the ears of C, (Fig.11, C1, C2 and C3) appear to be partially blanketed in ejecta from C suggesting that these pre date the formation of C itself.

The alignment of these feature could be viewed as a coincidence, with each structure (A, B and C) owing it's origin to a separate impact event. Certainly the Lunar Orbiter frame suggests that B has a somewhat different character to the more conventional looking A and C, but as with the example of the 'tadpole', an analysis of the ejecta blanket reveals the true nature of the 'Centipede'. The Clementine UV-VIS image of the area reproduced in Fig.12 shows that A, B and C, share the same, continuous ejecta blanket of finely comminuted debris, which appears consistent with a composition of immature, 'newly' exposed basaltic material. This ejecta is drawn out into fine rays that radiate off to the northwest and southwest, indicating a low angle impact from the east. Most conspicuous of all, are the thin elongate rays that appear to originate from crater C and extend westwards.

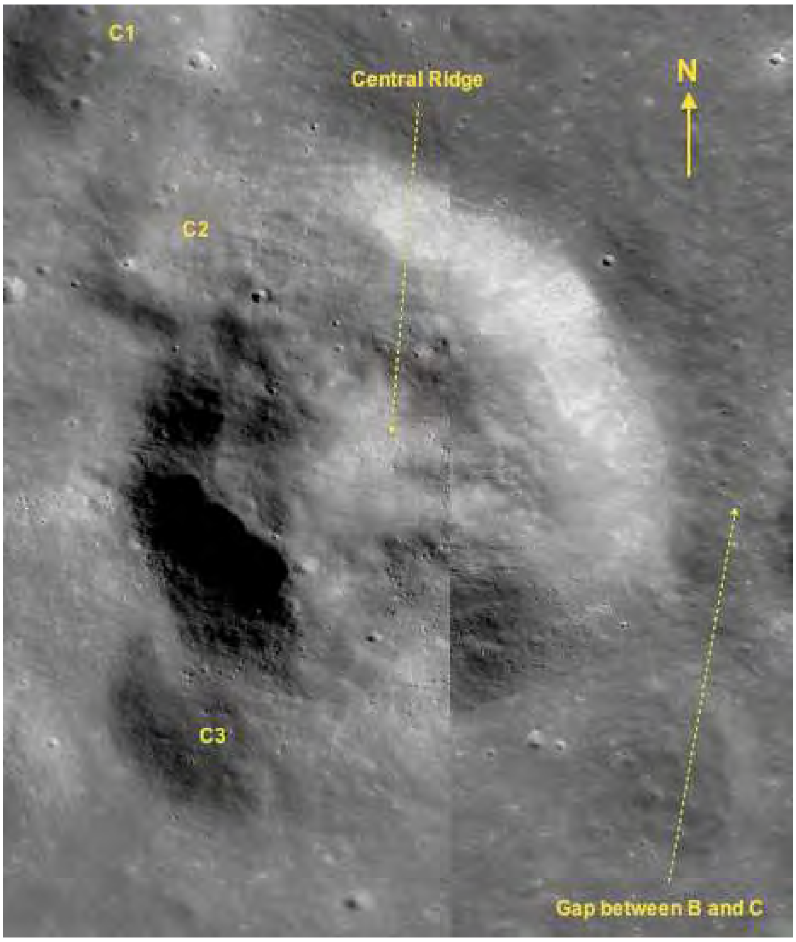

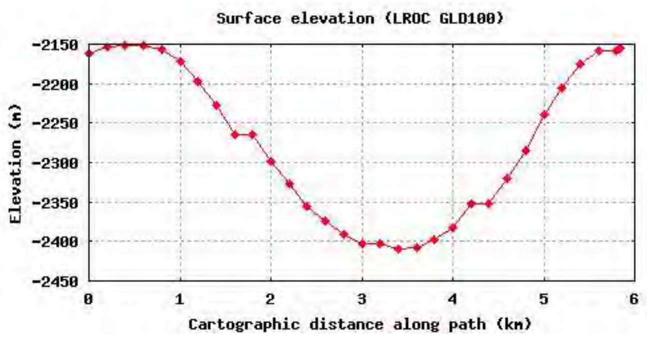

Fig.11 LRO image of crater C (above) and Topographic profile from west to east (below). Note craters C1, C2 and C3.

These rays give the structure the appearance of having long 'antenna' – hence the comparison with a centipede, and my nickname for the structure. One of these antenna can be seen to line up with the long axis of the whole structure and extend downrange towards Repsold R, (Fig.13) whilst a fine long ray extends to the northwest and a rather truncated one to the southwest. These rays can be seen to consist on fine lineations running parallel to the long axes of the rays, and possibly composed of numerous shallow overlying depressions caused by ballistic erosion during the impact process. Another fine ray can be seen to extend uprange, that is to the east, from crater A. This would appear inconsistent with a low angle impact from the east, but such up-range rays have been noted in other oblique angle impacts (Bell and Schultz 2012). The ejecta either side of B appears to take the form of a series of 'butterfly wings' which are characteristic of low angle impacts. One such wing, visible in the UV-VIS Ration Map image, and to the north of the widest section of B, can also be seen in the Lunar Orbiter image (marked EL in Fig.9) with a small impact crater superimposed upon it.

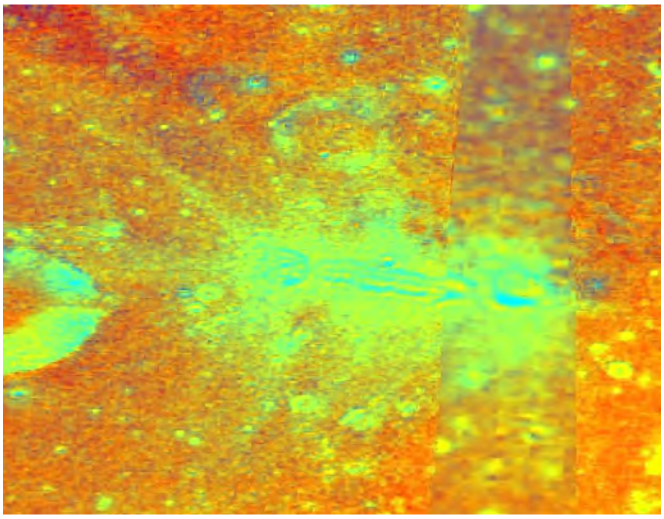

Fig.12 Clementine UV-VIS Ration Map image of 'Centipede' RGB bands 3.2.1 Repsold R is on the left of the frame.

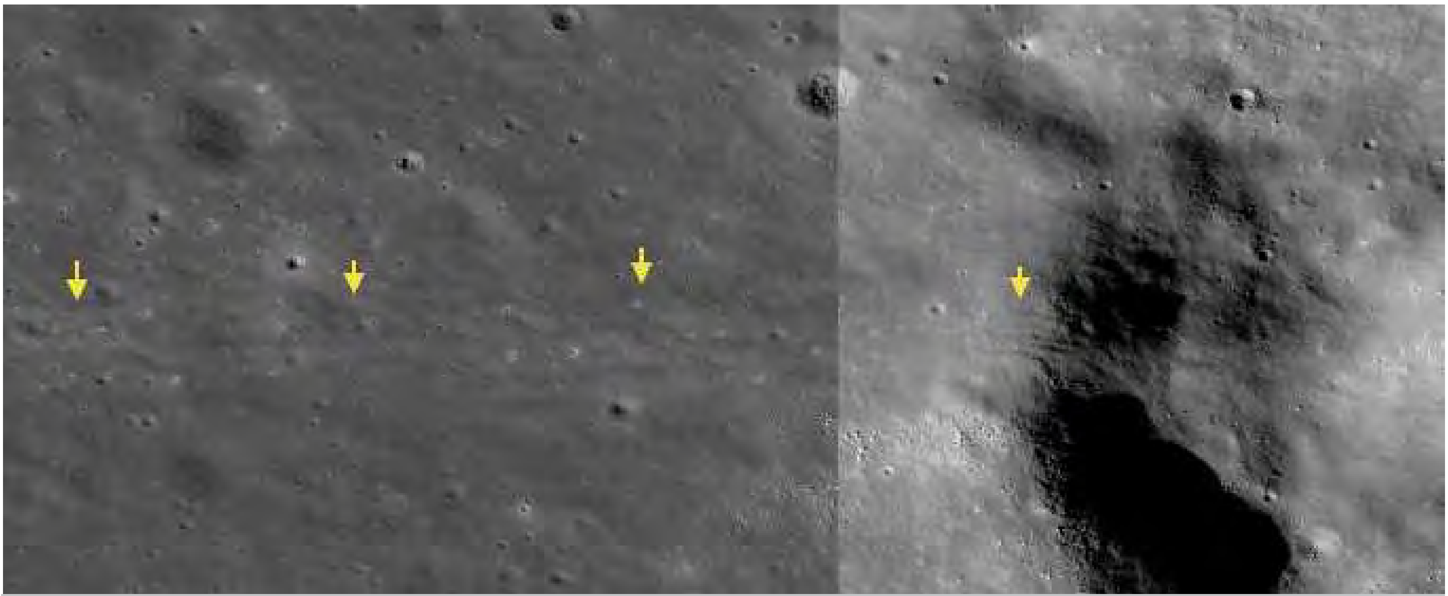

Fig.13 Detail of ray (indicated by arrows) extending from crater C towards Repsold R

These observations would suggest that this complete structure, craters A, B and C were formed in a single low angle impact event. The nature of the impact is however somewhat problematic, with a single point impact seeming unlikely.

It may be more likely that this structure was formed by a string of impactors, formed by a tidally disrupted small parent body, arriving from the east. The distribution of the ejecta as seen in the UV-VIS Ration Map image would suggest a simultaneous or near simultaneous impact for all projectiles, with the presence of a straight septa within B suggestive of such a process (Oberbeck 1973). The presence of the two separate 'normal' impact craters A and C with the elongate B between, would indicate a pair of impactors separated from each other by a string of smaller impactors in between, in something resembling a 'dumbbell' configuration. Research suggests that Earth Crossing Asteroids could be tidally disrupted to produce either strings of impactors – a 'string of pearls' as seen in Shoemaker 9 or a more condensed clump of three or more fragments with much of the mass condensed into the largest fragment (Bottke et.al, 1997). Could this latter type of mild disruption be responsible for the formation of the Centipede?

Another structure bearing a very similar morphology to the Centipede is Catena Littrow (Fig.14), an 11km long structure on the eastern shore of Mare Serenitatis, and composed of a number of separate craters arranged in an irregular chain.

A clear Zone of Avoidance to the west indicates an impactor trajectory from that direction, whilst the individual craters downrange exhibit the clear butterfly ejecta patterns of oblique impact. As with the 'Centipede', a number of transverse septa can be seen separating each smaller crater from it's neighbour.

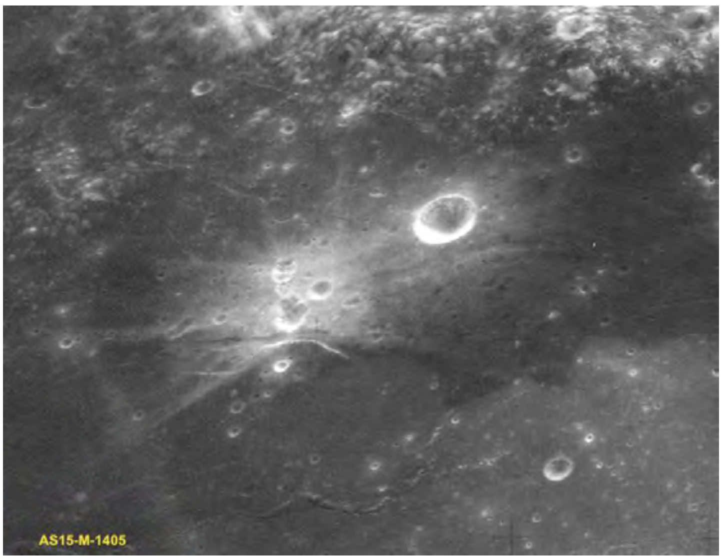

Fig.14 Catena Littrow showing the irregularly divided craters arranged in a loose chain. Apollo 15 image AS15-M-1405. Note the Zone of Avoidance in the ejecta towards the observer.

Each component crater appears irregular in planform and profile, with a superficial similarity to that seen in the 'Centipede', and it is also possible to see in places an apparent subdivision into smaller elements (Fig.15). A topographic profile strengthens the similarity between this structure and the 'Centipede', by showing that the craters at each end of the Catena deeper than those in between (deepest in the west, shallowest in the east) possibly indicative of the simultaneous but separate impact of two larger fragments of a disrupted body, with the smaller, shallower craters in between being formed by intervening debris. The irregular nature of these craters may suggest a friable and fragmentary group of impactors following the tidal disruption of a 'rubble pile' body of low inherent tensile strength. The analogy used above of a shotgun blast as opposed a rifle bullet may be pertinent in these cases.

One final example may serve to illustrate this suggestion, with Fig16 showing a 3km long structure some 80 kms to the west of Flamsteed Z. This is composed of a loose chain of craters, with small sub circular craters at each end separated by a irregular field of shallower, offset depressions. These contrast strikingly with a number of small (approximately 10-30m in diameter) simple impact craters on the adjacent mare surface, and suggest a differing impact dynamics which may be a consequence of impactor composition and friability. Again, the presence of larger impacts at either end may suggest the involvement of a tidally disrupted impactor.

All of the above structures are significantly smaller than the most prominent crater chain, Catena Davy. The individual craters in the Davy Chain appear discrete and regular in outline and depth as compared to the irregularity seen in the above examples, and Wichman and Wood (1995) argue strongly for their origin as primary and not secondary impacts. Davy G is not considered part of the chain by many lunar students(Bottke, et.al 1998) and is not shown as being related in the LAC Chart (Howard and Masursky 1968) but the alignment of this crater with the chain may be more than coincidence.

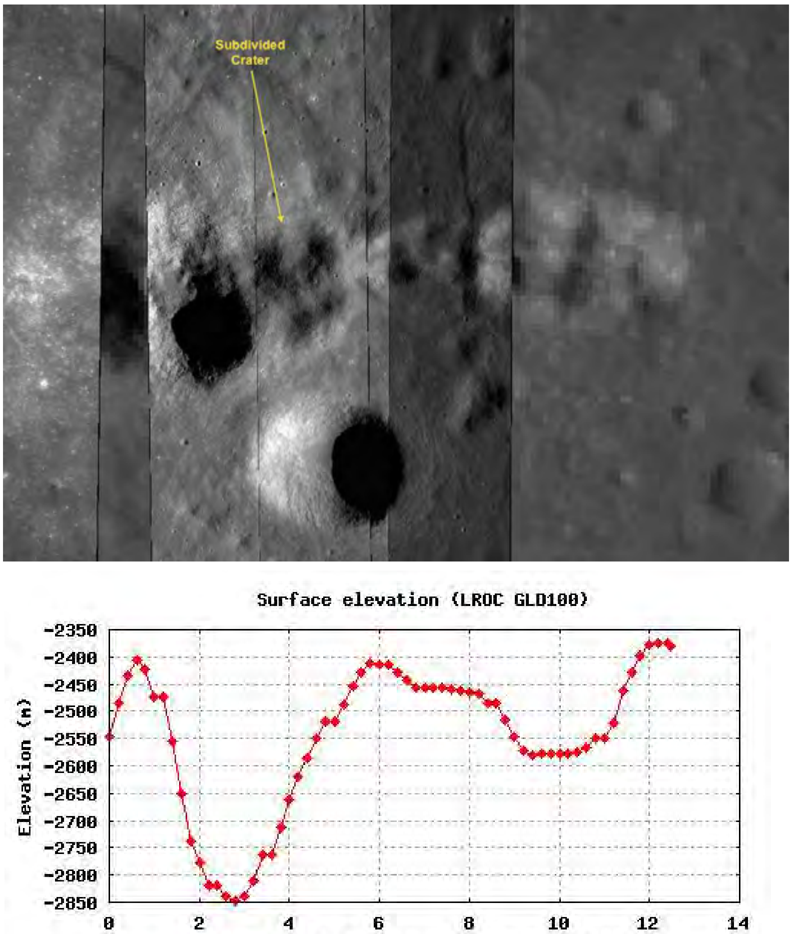

Fig.15 LRO image of Catena Littrow, with Topographic profile (below) showing the separation of the feature into two main components. Note the irregular crater floors along the length of the Catena and apparent subdivision of some craters in the chain.

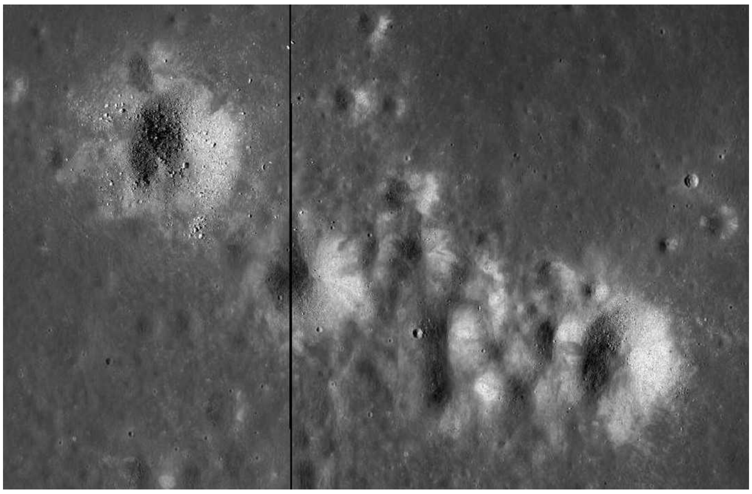

Fig.16 LRO image of impact structure 80kms west of Flamsteed Z. Note the rather more conventional looking craters at either end of the chain and the irregular impact structures between. These contrast strikingly with the smaller impact craters visible nearby.

In Fig.17 we can see that the LRO Topographic profile of Davy G strongly indicates an oblique impact origin, with the 'up range' inner western wall being much steeper that the 'down range' eastern wall. The axis of symmetry of Davy G (line X – Y) coincides with the line of the crater chain, highly suggestive of a common origin in the impact of a line of debris following behind a larger parent body. One must not rule out a chance alignment, these can and do occur on the moon, and play to an observers predisposition for linking unrelated structures. In this case however, the orientation of the ejecta from the craters in the chain suggest an origin in a line of impactors travelling along a west to east trajectory. The morphology of Davy G also suggests an origin during the impact of a body travelling along an identical trajectory. This observation together with the coincidence of the long axes of the chain and Davy G reinforces the case for a common origin.

It may be possible to surmise from the above observations that the role of tidal disruption of NEA's has a part in the production of a broad family of crater chains on the moon. The low probability of the production of Davy Chain type structures (Bottke, et.al, 1997) may not reflect the frequency of disruption of smaller bodies which go on to form the crater chains discussed above. In addition, the irregular crater planforms observed in this population of smaller chains, together with their restricted linear extent indicate a rather milder disruption of a population of small 'rubble pile' type body of low tensile strength.

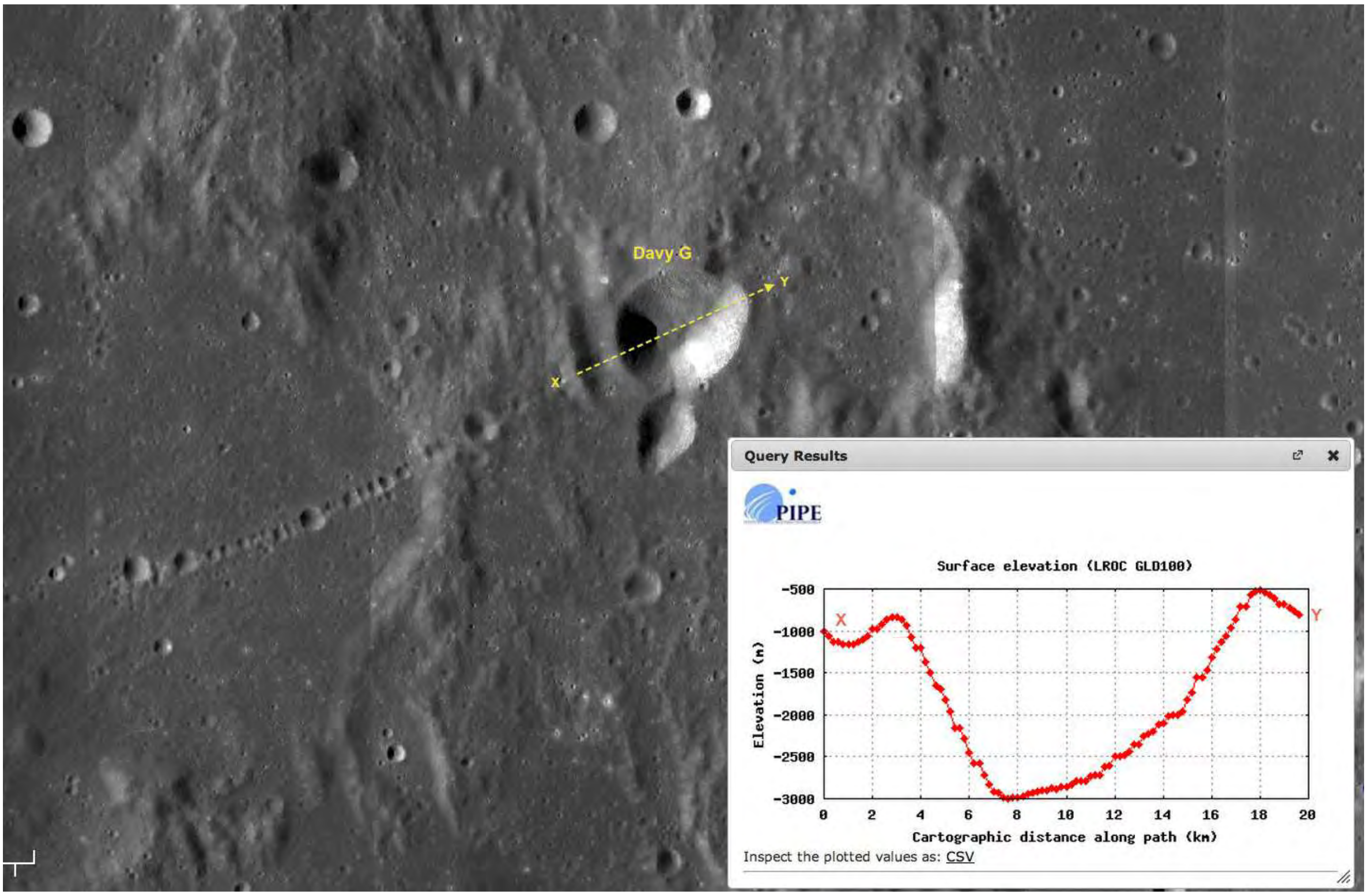

Fig.17
The Davy crater chain and Davy G with LRO Topographic Profile along line X-Y

Selenology Today

References

Bell, S.W and Schultz, P.H, 2012. DETECTION OF A RADAR SIGNATURE OF THE UPRANGE PLUME IN FRESH OBLIQUE LUNAR CRATERS. 43rd Lunar and Planetary Science Conference (2012)

Bottke,W.F, Richardson,D.C and Love,S.G. 1997 Can Tidal Disruption of Asteroids Make Crater Chains on the Earth and Moon? Icarus, Volume 126, Issue 2, pp. 470-474

Bottke,W.F, Richardson,D.C and Love,S.G. 1998 Tidal Distortion and Disruption of Earth-Crossing Asteroids. Icarus Volume 134, 47–76.

Howard, K.A and Masursky, H, 1968 Geological Map of the Ptolemaeus Quadrangle of the Moon. US Geol. Survey Misc Geol. Map I-566 (LAC77; RLC13)

Oberbeck, V. R, 1973 Simultaneous Impact and Lunar Craters.The moon, Volume 6, Issue 1-2, pp. 83-92

Wichmann, R.W and Wood, C.A, 1995 The Davy Crater Chain: Implications for tidal disruption in the Earh-Moon system and elsewhere. Geophysical Research Letters, Vol.22, pp 583 - 586

Acknowledgements

LROC images and topographic charts reproduced by courtesy of the LROC Website at http://lroc.sese.asu.edu/index.html, School of Earth and Space Exploration, University of Arizona.

Fig.9 and 14 courtesy Lunar and Planetary Institute web site at http://www.lpi.usra.edu

Fig.5 courtesy of the USGS PSD Imaging Node at http://www.mapaplanet.org/

Note: This article is based on a shorter one previously submitted to the BAA Lunar Section for inclusion in their monthly newsletter.

Selenology Today

Moretus and the southern lunar region

Richard Hill
(Jim Loudon Observatory)

On August 25 2012 at 02:10 UT, I imaged the region around Moretus. Fig. 1 displays a mosaic of 4 images. I noticed that from the north rim of Moretus east through the shared rim of Simpelius and Simpelius A and a little farther east ending at Simpelius G is what appears to be a "fault" of some sort. The feature is shown with arrows in the corresponding Fig.2.

Fig.3 displays one of the 4 frames that shows most of the feature. Note the shadow between Simpelius and Simpelius A. For this four image montage I used Registax6, GIMP and Irfanview in processing the images and combined them with AutoStitch.

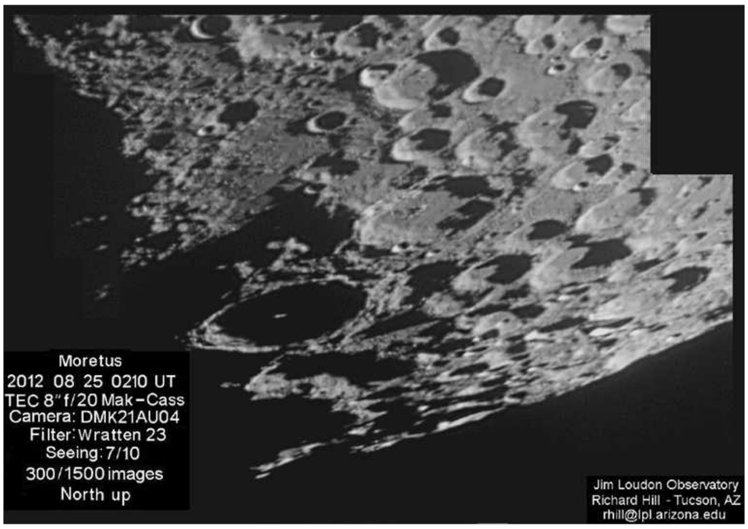

Fig.1

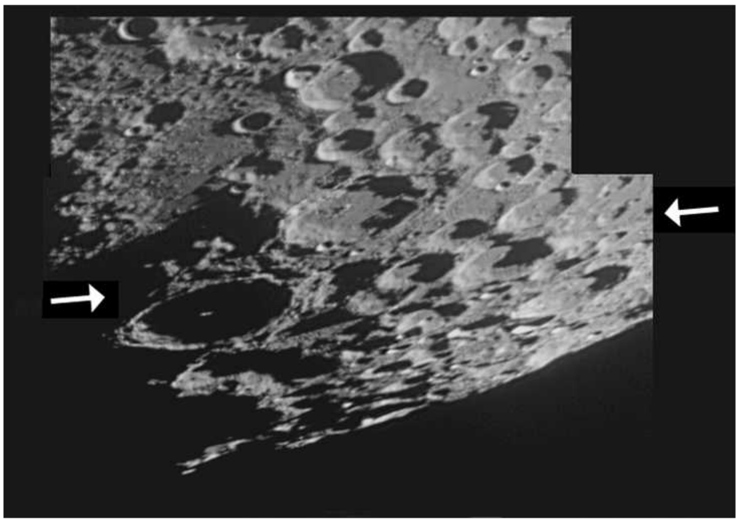

Fig. 2

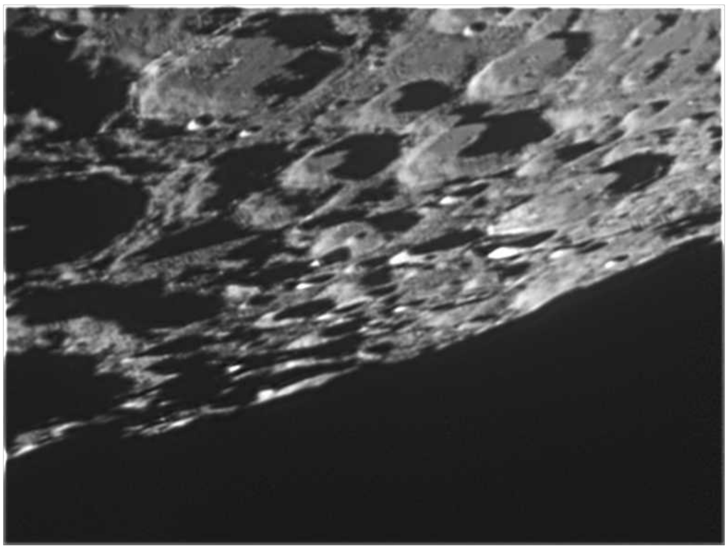

Fig. 3

Selenology Today

It seems rather obvious once you see it and seems quite real with that shadow between Simpelius and Simpelius A adding to the appearance. This feature does not appear as a named feature in the Rukl Atlas, Virtual Moon Expert nor MROC and on the latter it appears it could be raised areas roughly aligned because of the juxtaposition of the neighboring crater rims. Fig.4 shows a crop of the LRO WAC imagery where lineation is visible in this rugged region. It looks like it's a chance alignment of crater rims, scarps, and as in the case of the area just west of Simpelius E and D, some general topographic textural changes. Of course in the lower resolution of my images it looks very real as a valley.

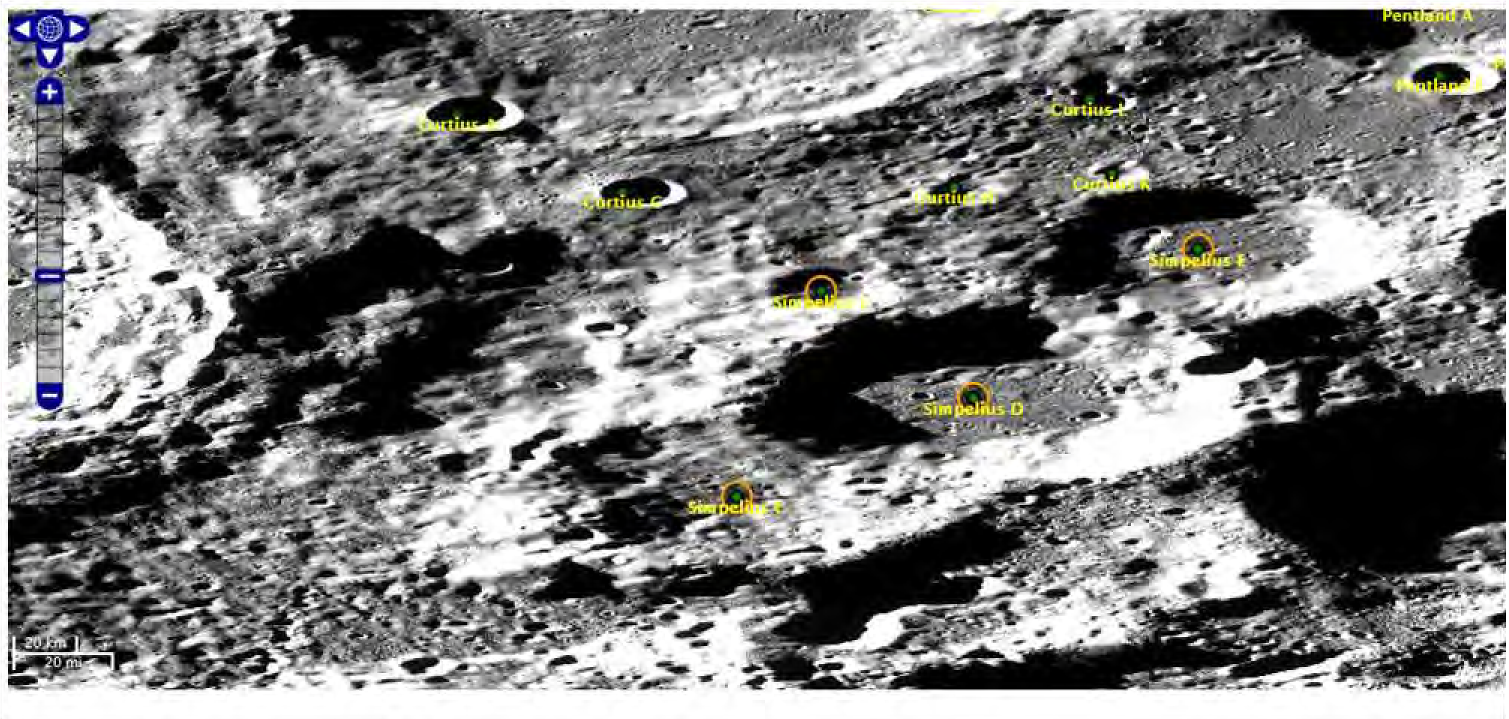

Selenology Today

Lunar Kipuka in Opelt

Raffaello Lena and Maurizio Morini
GLR group

Abstract

In this paper is described a lunar kipuka located near the crater Opelt. The nature of the large feature is identified using spectral map and crater counts, demonstrating it is older than surrounding mare lavas. Based on GLD 100 data, the kipuka rises at 530 m over the surrounding mare.

Introduction

The term kipuka indicates elevated "islands" surrounded by the flooding mare lavas. Kipukas usually consist of a different material than the surrounding mare, such that a spectral contrast is observed. A typical example of a lunar kipuka is the formation Darney χ located in western Mare Cognitum, an elevated section of highland terrain embayed by mare lava (Nichols et al. 1974).

In general the kipukas show rilles crossing their summit, indicating structural control by subsurface geology and these features are commonly interpreted as fractural features that may occur as a result of the flexural uplift (Nichols et al. 1974).

In this article the presence of a lunar kipuka, located near Opelt, at the boundary of mare Cognitum and Nubium, is discussed, including a comparison with Darney χ.

Ground based observation and Clementine spectral data

The images shown in Figs 1 and 2 (including LRO excerpt) have been made on March 31 2012 at 21:40 UT using a Mak-Cassegrain 18 cm.

Several rilles are traversing the summit of the large feature, which is a kipuka for two reasons related to:

a) different spectral contrast and different material;

b) difference in crater counts.

The Clementine UV-VIS image of the area, shown in Fig. 3, displays an evident different spectral appearance. The domical object appears spectrally consistent with an older material, red in the UV-VIS maturation false color map. Furthermore, it (with a diameter estimated of 52 km) is more fractured and more pitted with smaller craters demonstrating that it is older than the surrounding mare lavas (cf. Fig.2 top right LRO excerpt). The fact that the rise is cut by fractures suggests that its elevation may have resulted from it being domed upward.

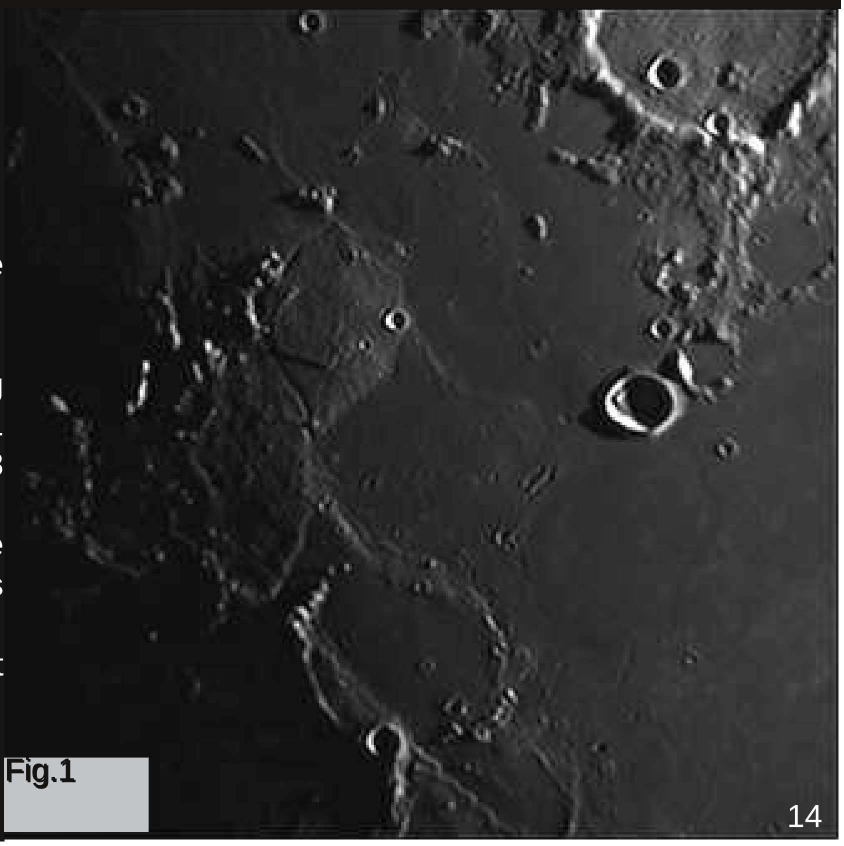

Fig.1

Selenology Today

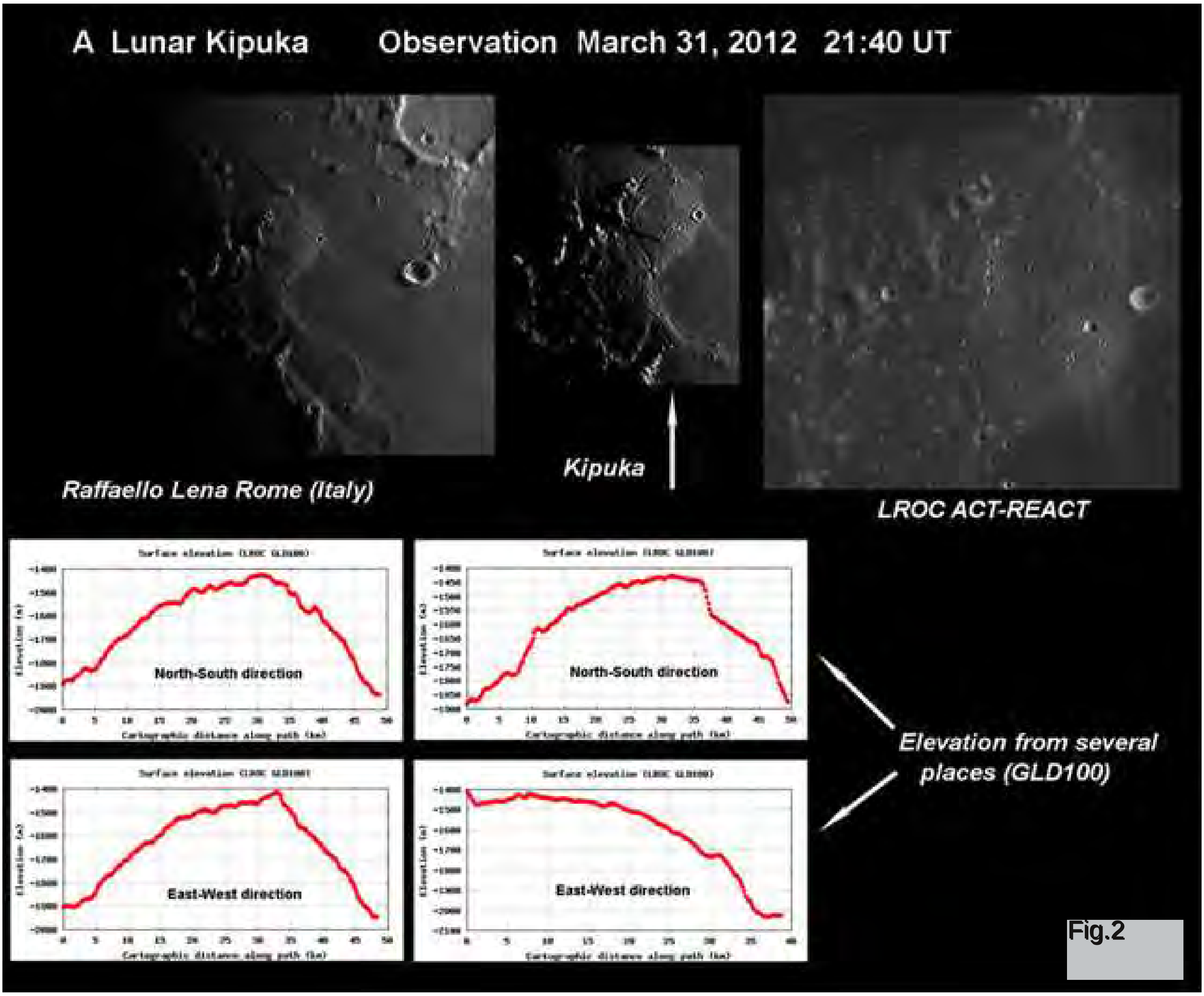

Fig.2

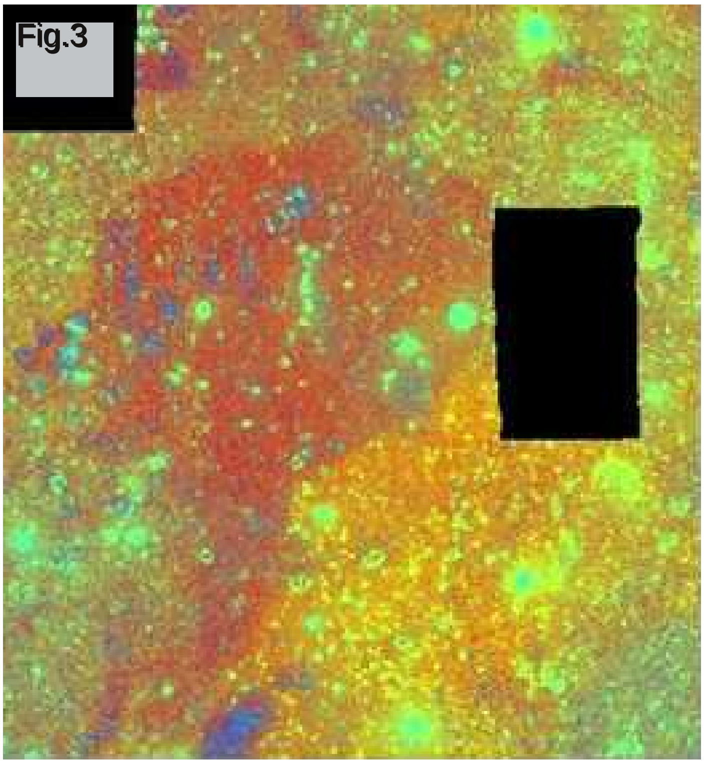

Fig.3

GLRGROUP.org
Geological Lunar Researches Group

Selenology Today

Spectral properties

Compared to the Darney χ.formation (cfr. Fig 4 for the region of interest), the examined kipuka displays a similar albedo at 750 nm (0.13-0.14) and a higher R415/R750 ratio (0.59 vs. 0.56). Based on Clementine UVVIS+NIR multispectral imagery, we furthermore determined the continuum slope of the spectrum, the width of the ferrous absorption trough around 1000 nm, and the wavelengths and relative depths of the individual absorption minima and inflection features. The kipuka displays a single absorption at 970-980 nm (depth 6.4%), indicating the presence of high-Ca clinopyroxene. Darney χ is a light plains unit while Darney τ is composed of a series of hills (Fig.4).

Elemental abundances and petrographic analysis

We estimated the abundances of the elements Ca, Al, Fe, Mg, Ti, and O based on the previously extracted spectral features, mapping them to Lunar Prospector gamma ray spectrometer data using the second-order polynomial regression method introduced by Wöhler et al. (2011). Furthermore, we determined the petrographic maps, which indicates the relative fractions of the three endmembers mare basalt (red channel), Mg-rich rock (green channel), and ferroan anorthosite (FAN, blue channel) as proposed by Berezhnoy et al. (2005). The red to orange colour in the petrographic map (Fig. 5) indicates the presence of a mare basalt composition. The blue coloration indicates very low iron rock, consistent with ferroan anorthosite or generally highland-like material. The green colour indicates the presence of magnesium rich rock and is sensitive to the presence of olivine. The light purple colour shows a mixture of highland material (blue) and mare basalt (red). To distinguish between different mare basalt types in the examined region, we produced another petrographic map which displays the relative fractions of the three basalt end-members titanium poor mare basalt (red channel; 9.25 wt% Al, 1.6 wt% Ti), highland like-material (green channel; 14 wt% Al, 0.5 wt% Ti), and titanium-rich mare basalt (blue channel; 6.3 wt% Al, 3.6 wt% Ti). The relative fractions were inferred from a ternary diagram in the space spanned by the Al-Ti abundances.

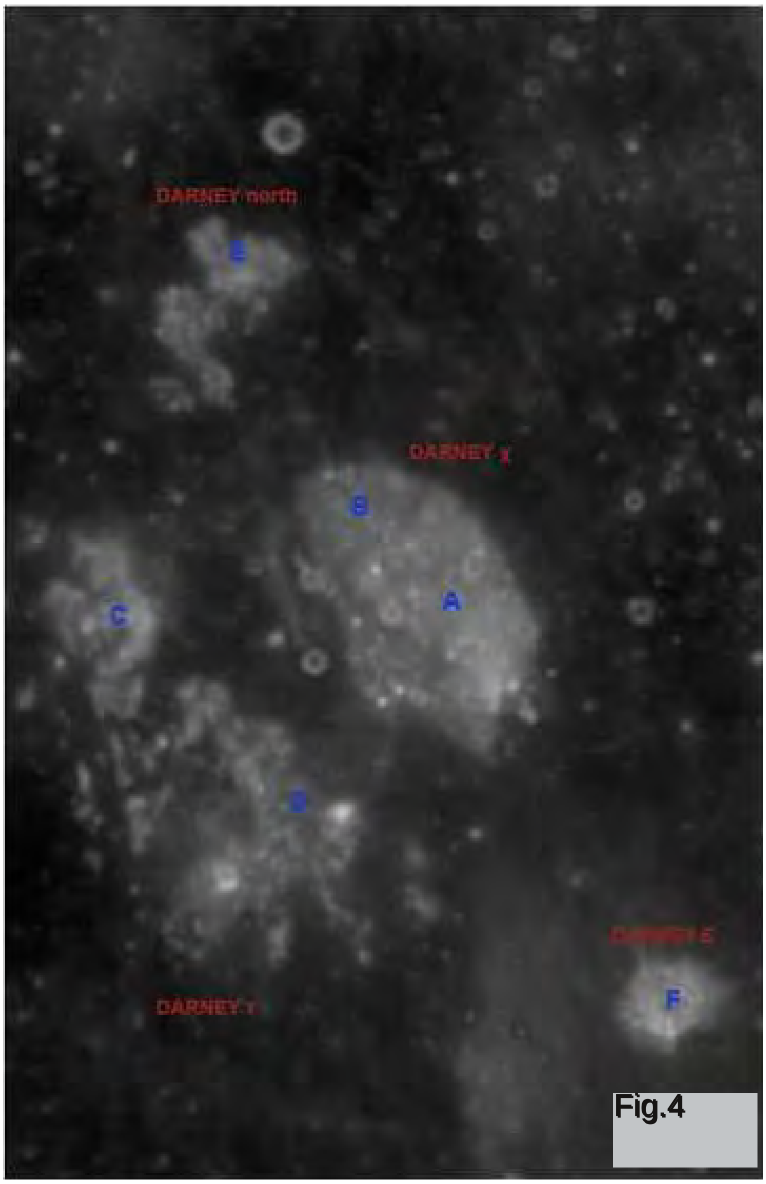

Fig.4

The examined kipuka appears as an “island” of highland material (blue) surrounded by mare basalt (Fig. 5). According to Table 1, it is rich in Ca and Al. The central region of the examined feature has a Fe content of 7.9% and a Ti abundance of 0.9 %. Nearby mare units are much richer in Fe and Ti, inferred as 11% and 1.5% respectively. Moreover some eastern parts of the kipuka exhibit higher Fe and Ti values due to admixed mare material.

The map shown in Fig. 6 reveals the corresponding green colour corresponding to a highland material.
Five near-IR spectra were obtained for Darney formation (Table 1), and exhibit absorption features (depth = 5% - 6.5%) that are centered between 970 nm and 990 nm. Examination of the corresponding petrographic maps of the Darney formations (cfr. Fig. 4 and Figs. 7-8) prepared using the Clementine UVVIS-NIR dataset reveal a highland composition. Moreover some regions appear as a mixture between mare basalt and highland material, according to preceding studies by Hawke et al. (2002). Furthermore Darney E crater has a relatively deep absorption band (depth = 15.5%) centered a 970 nm with Fe values of 16.3% and Ti values of 2.5%.

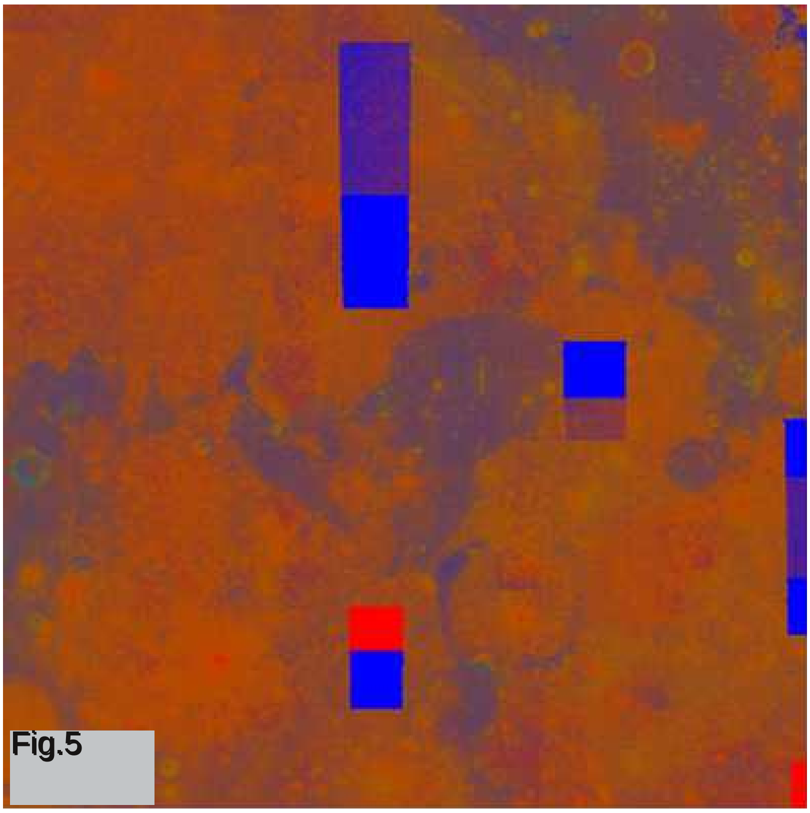

Fig.5

Table 1

Description	Fe %	Mg %	Ca %	Ti %	Al %	O %	BCW (nm)	DEPTH(%)	FWHM(nm)	750	415/750	950/750
Darney Chi centre	7,64	5,97	10,93	0,91	12,55	44,94	979,9	6,3	202,8	0,140	0,567	1,058
Darney Chi north	7,99	5,98	10,69	1,06	12,22	44,88	984,7	5,1	210,3	0,131	0,562	1,062
Darney Tau north	7,99	6,17	10,77	0,98	12,31	44,85	978,3	6,4	214,4	0,135	0,569	1,058
Darney Tau south	8,46	6,27	10,50	1,13	11,95	44,74	969,8	5,6	227,7	0,123	0,574	1,060
Darney North	7,63	5,81	10,95	0,95	12,52	44,95	989,9	5,8	191,2	0,129	0,571	1,069
Darney E crater	16,26	9,57	9,36	2,56	8,09	41,92	972,5	15,5	285,5	0,151	0,627	0,916
Kipuka centre	7,88	6,05	10,87	0,97	12,40	44,86	980,42	6,43	196,00	0,129	0,594	1,063
kipuka eastern part	9,33	6,76	10,14	1,29	11,41	44,48	964,53	6,33	250,70	0,130	0,603	1,042
Mare unit east	11,03	7,62	9,62	1,55	10,42	43,95	974,94	8,95	304,03	0,115	0,578	1,029

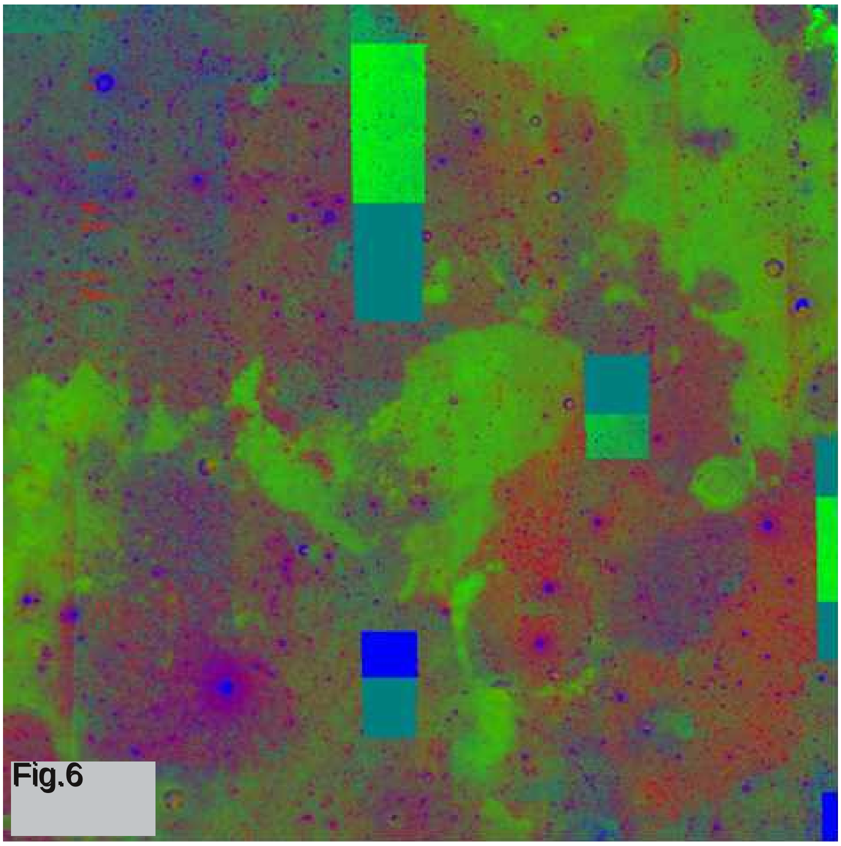
Fig.6

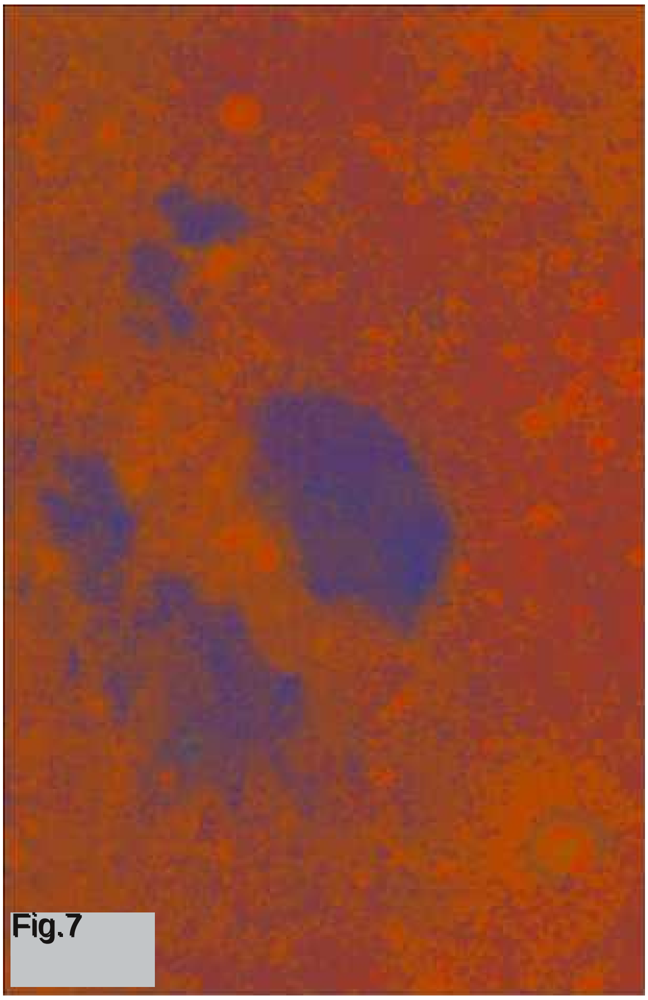
Fig.7

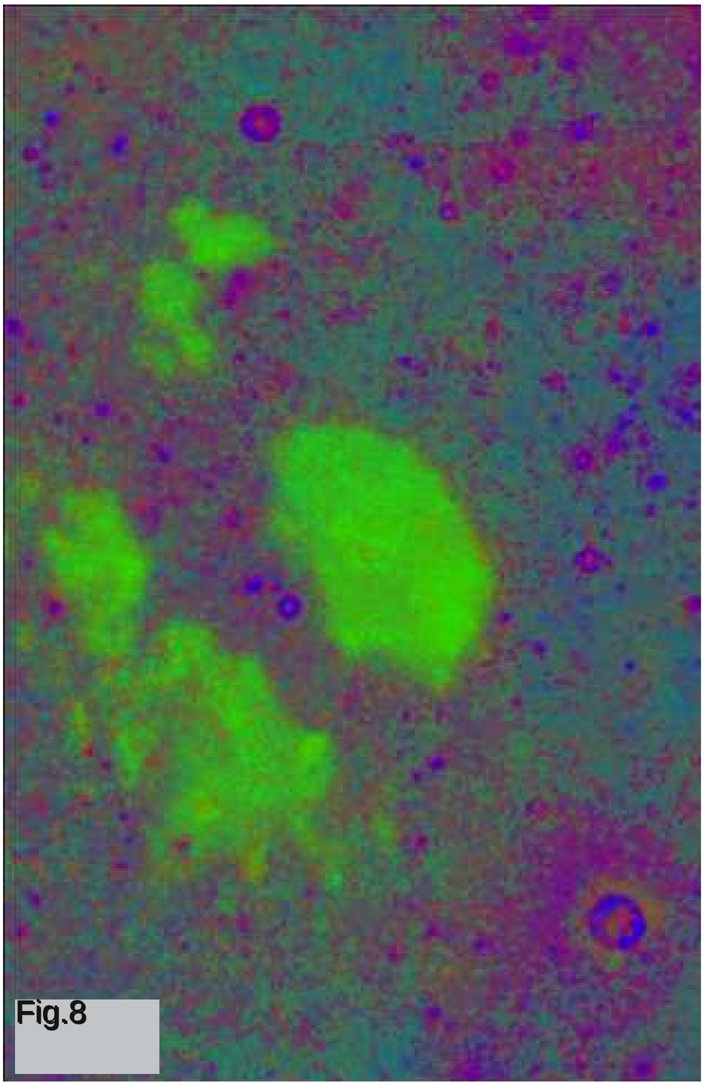
Fig.8

Selenology Today

LOLA DEM

Recently, a global lunar digital elevation map (DEM) obtained with the Lunar Orbiter Laser Altimeter (LOLA) instrument on the Lunar Reconnaissance Orbiter (LRO) spacecraft has been released (http://pds-geosciences.wustl.edu/missions/lro/lola.htm).
A rendered image obtained using LTVT software package by Mosher and Bondo (2010) and the LOLA DEM, and assuming the same illumination conditions as in Fig. 1, is shown in Fig. 9. In the LOLA DEM, the elevation difference between the centre and the eastern border amounts to about ~530 m, yielding for highest hills elevation of 740 m, which is in a good agreement with our image-based photoclinometry and shape from shading analysis.

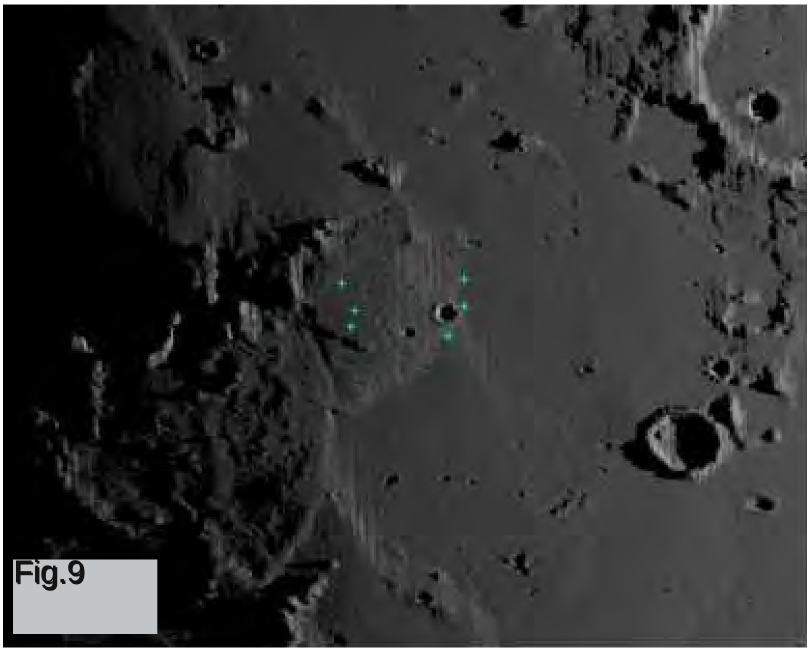
Fig.9

GLR 100 data

Using digital photogrammetric techniques, a terrain model can be computed from the stereo overlap and a useful web resource is represented by the LRO altimetry tool (ACT-REACT Quick Map). Using this data set it is possible determine distances, profiles, depths and/or elevation of several lunar features. Using the ACT-REACT tool, GLD 100 data, the kipuka is rising at about 500 m in North-South direction. Similar elevation was derived also for the East-West directions, as shown in Fig. 10.
Furthermore, the green line indicates the location of the cross-sectional profile shown in Fig. 11, where an elevation of 530 m was computed, resulting in a flank slope of 1.1°.
A comparison with typical example of a lunar kipuka corresponding to the formation Darney χ was employed. Compared to the surrounding dark mare, the surface of Darney χ is older because it has more large craters and is crossed by almost eroded rilles.
Using the ACT-REACT tool, GLD 100 data a dimension of 21 x 15 km was computed.
The green lines indicate the location of the cross-sectional profiles, shown in Figs. 12-13, where an elevation of 100 m was computed, resulting in a flank slope of 0.65°. Hence, the examined lunar kipuka, traversed by the Opelt rille, has higher elevation than Darney χ.

References

Berezhnoy, A. A., Hasebe, N., Kobayashi, M., Michael, G. G., Okudaira, O. & Yamashita, N., 2005. A three end-member model for petrologic analysis of lunar prospector gamma-ray spectrometer data. Planetary and Space Science 53:1097–1108.

Hawke, B. R., Lawrence, D. J., Blewett, D. T., Lucey, P. G., Smith, G. A., Taylor, G. J. and Spudis, P. D., 2002. Remote sensing studies of geochemical and spectral anomalies on the nearside of the Moon. Lunar and Planetary Science XXXIII, abstract 1598.

Mosher, J., & Bondo, H., 2010. Lunar Terminator Visualization Tool.
http://ltvt.wikispaces.com/LTVT+Download
(last accessed July 29, 2012)

Nichols, D. J., Young, R. A. & Brennan, W. J., 1974. Lunar kipukas as evidence for an extended tectonic and volcanic history of the maria. Lunar Planet. Sci. V, pp. 550–552.

Wöhler, C., Berezhnoy, A., Evans, R., 2011. Estimation of Elemental Abundances of the Lunar Regolith Using Clementine UVVIS+NIR Data. Planetary and Space Science 59(1), pp. 92–110.

Selenology Today

North-South direction

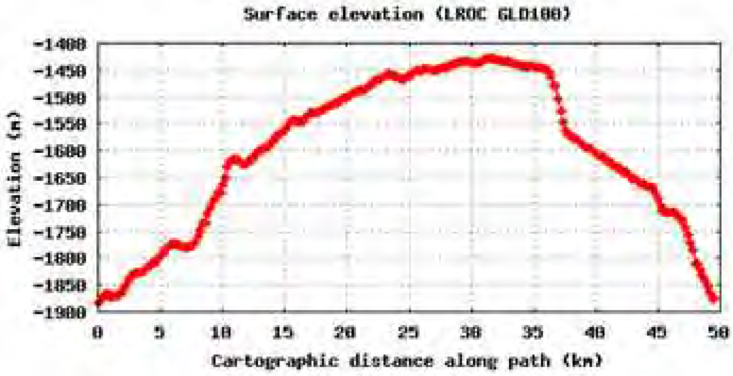

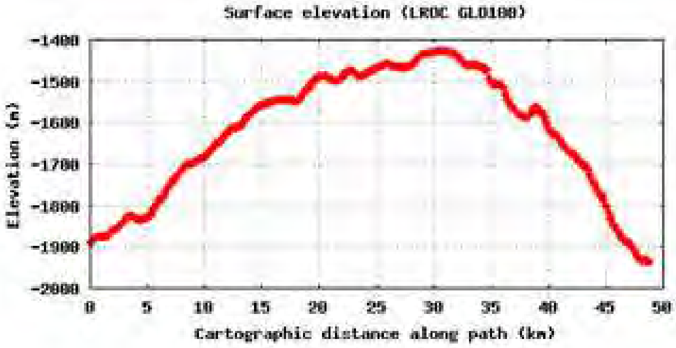

East-West direction

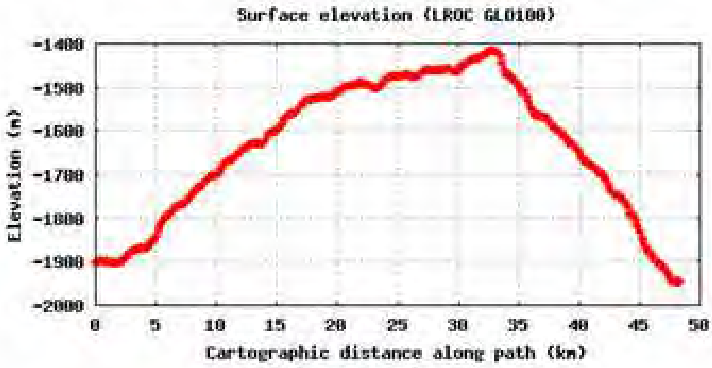

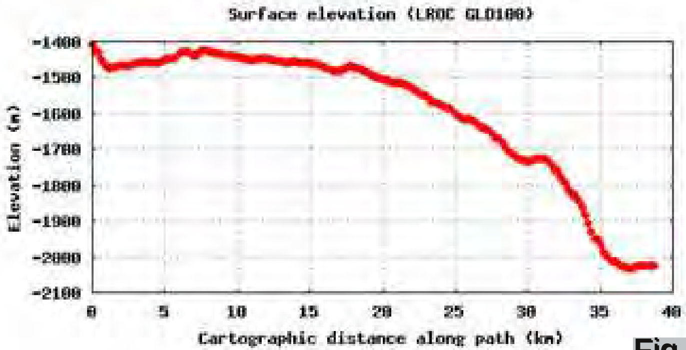

Fig.10

Selenology Today

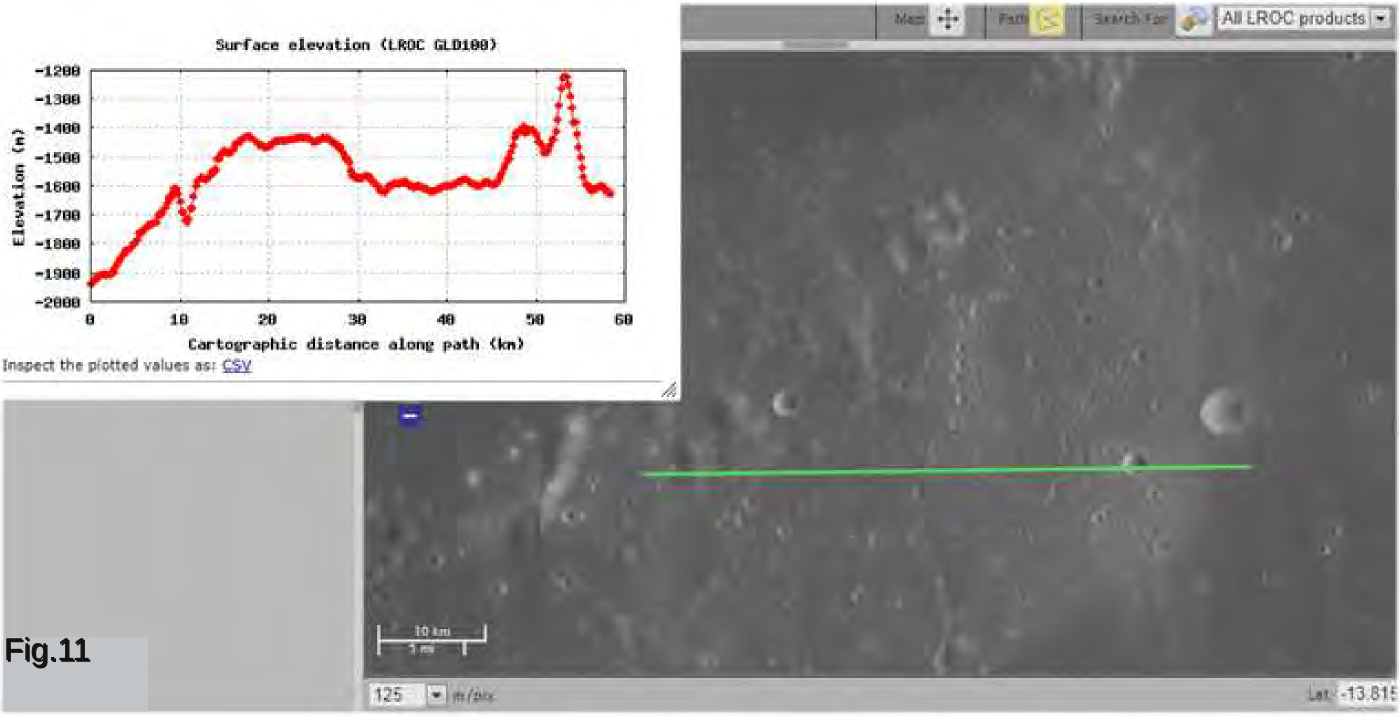

Fig.11

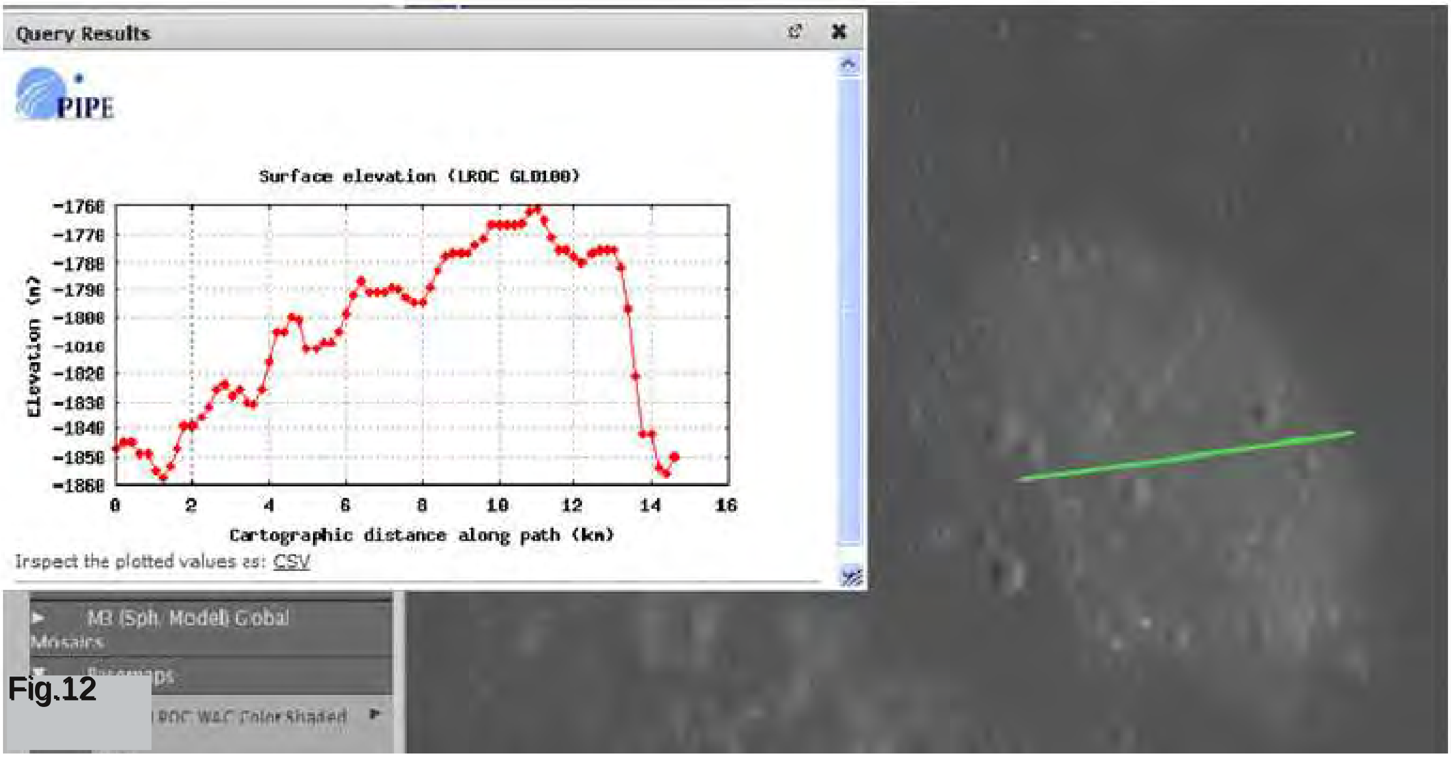

Fig.12

Geological Lunar Researches Group

Selenology Today

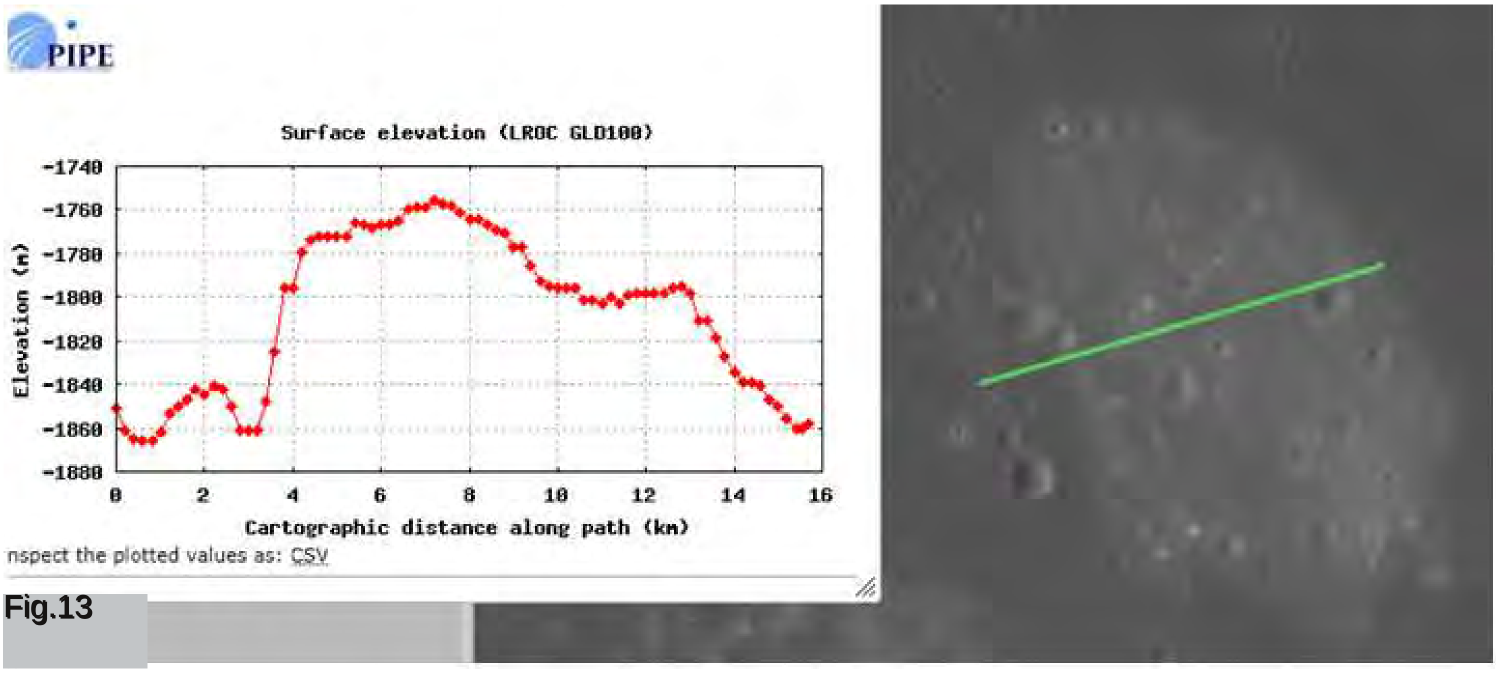

Fig.13

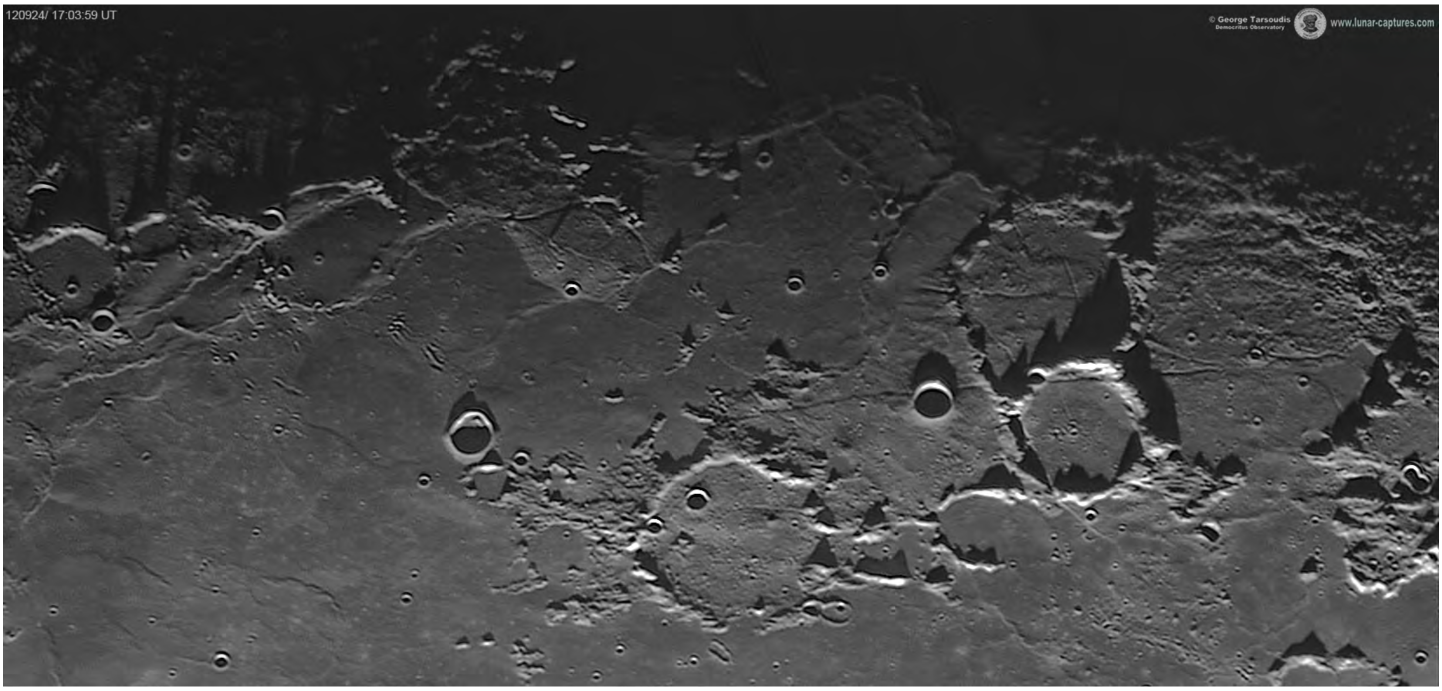

Image from the area of the **Lunar Kipuka** by George Tarsoudis (24 Sep. 2012 / 17:03 UT), Telescope 10 inch @f/6.3, camera Unibrain fire-i 785, filter Red, barlow 3X.

GLR GROUP.org
Geological Lunar Researches Group

Selenology Today

Lunar Occultation of Jupiter and Venus occurred during July and August 2012

During the early hours of July 15, 2012 the waning Moon occulted the planet Jupiter for many observers in Europe and North Africa. It was a difficult event due to the low height of the Moon in the sky. Another occultation occurred on August 13, 2012: the waning Moon occulted a half lit Venus for many observers in North America. Some reports and images were received and they are presented here.

Philips Jennings (UK)

I got a few images using a camera on a tripod. Here in the north-west of England it was an extremely close conjunction rather than an occultation, but it was beautiful nevertheless.

Selenology Today

George Tarsoudis (Greece)

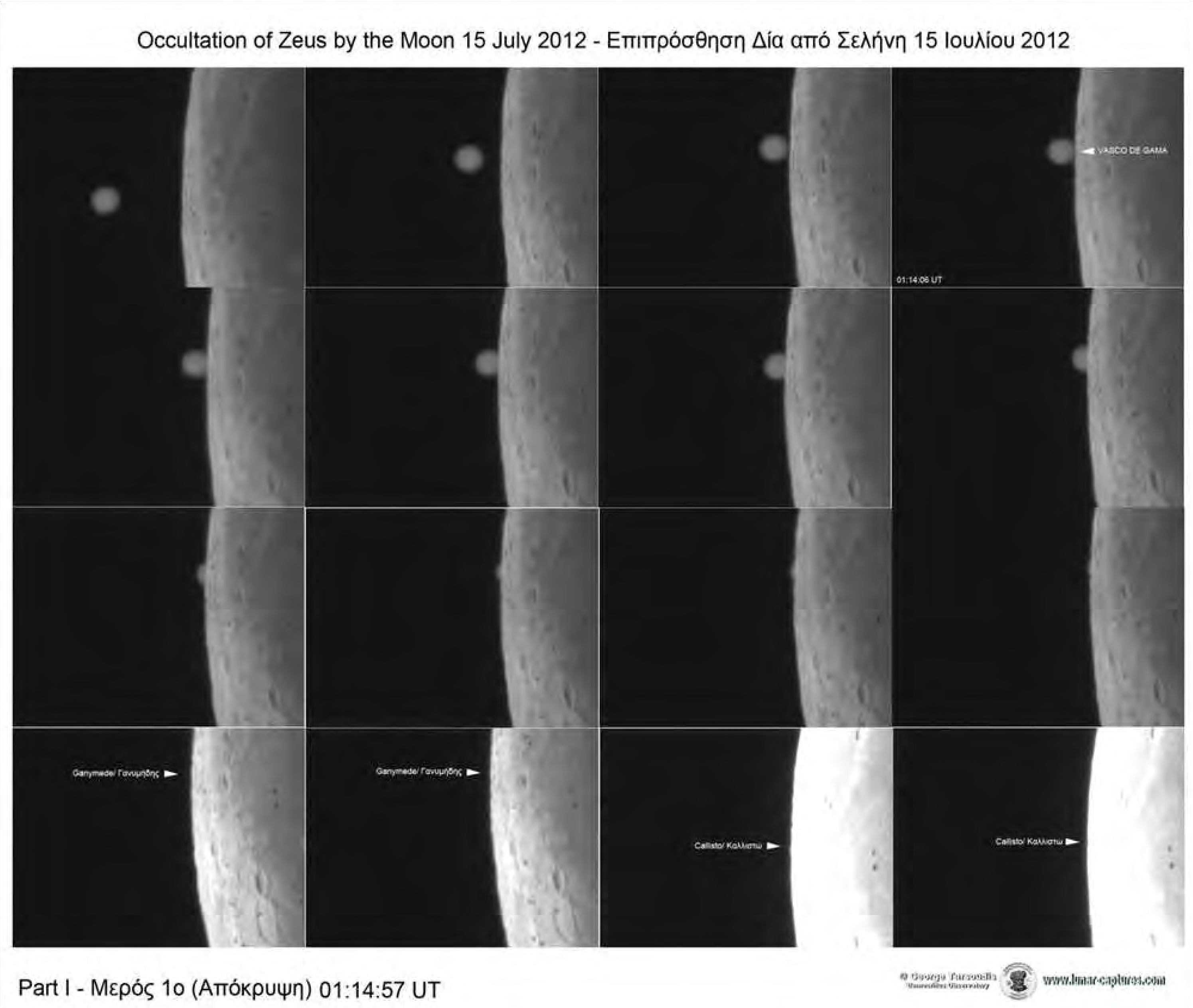

From Alexandroupolis the Occultation of Zeus (Jupiter) and its moons by the Selene. Equipment TSA 102N, DMK 21AF04, barlow 3X, filter Red. Two phases ingress and egress are presented.

Selenology Today

George Tarsoudis (Greece)

Occultation of Zeus by the Moon 15 July 2012 - Επιπρόσθηση Δία από Σελήνη 15 Ιουλίου 2012

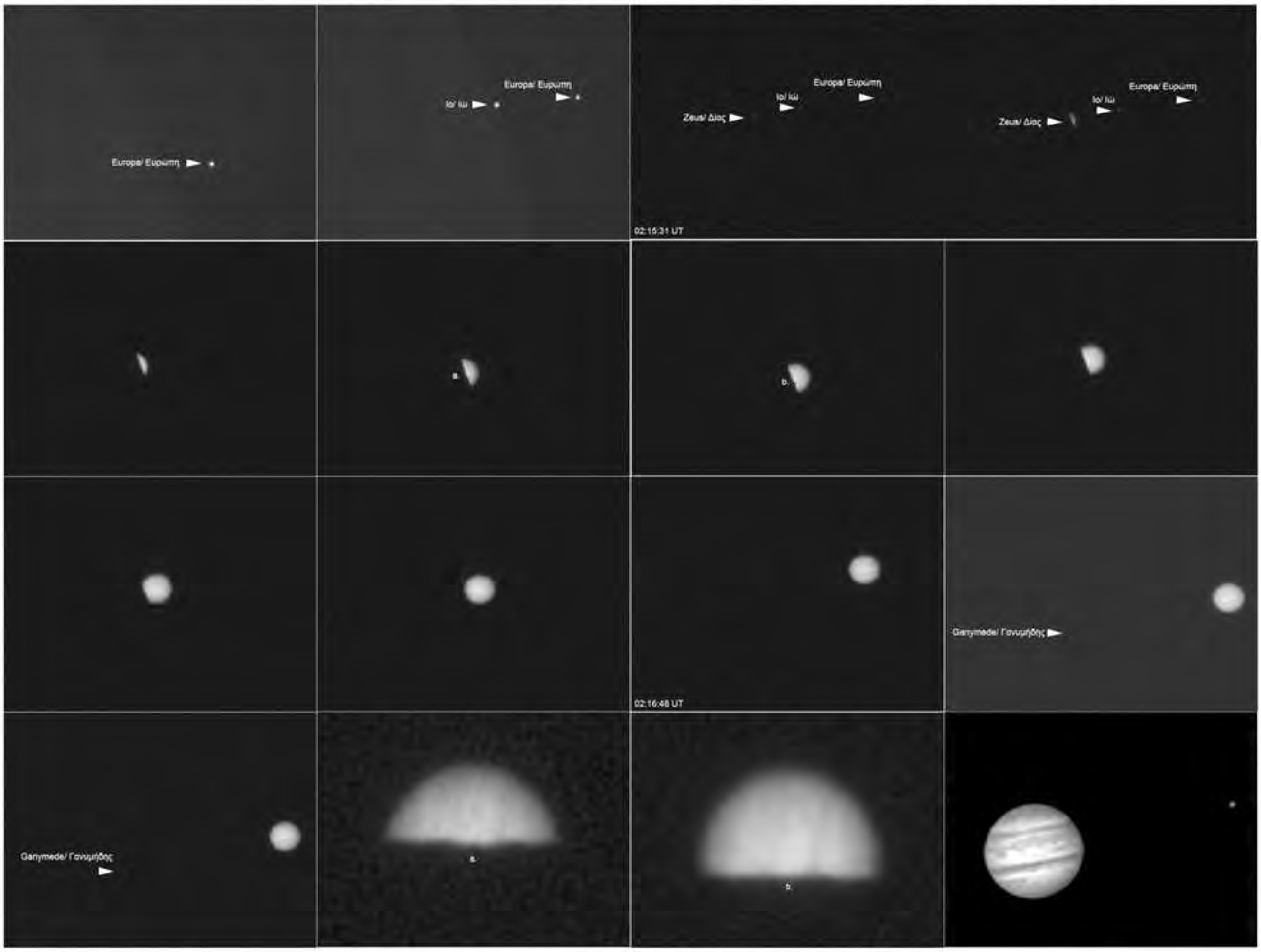

Part II - Μερός 2ο (Επανεμφάνιση) 02:15:31 UT

© George Tarsoudis www.lunar-captures.com

Selenology Today

Raffaello Lena and Maria Teresa Bregante (Italy)

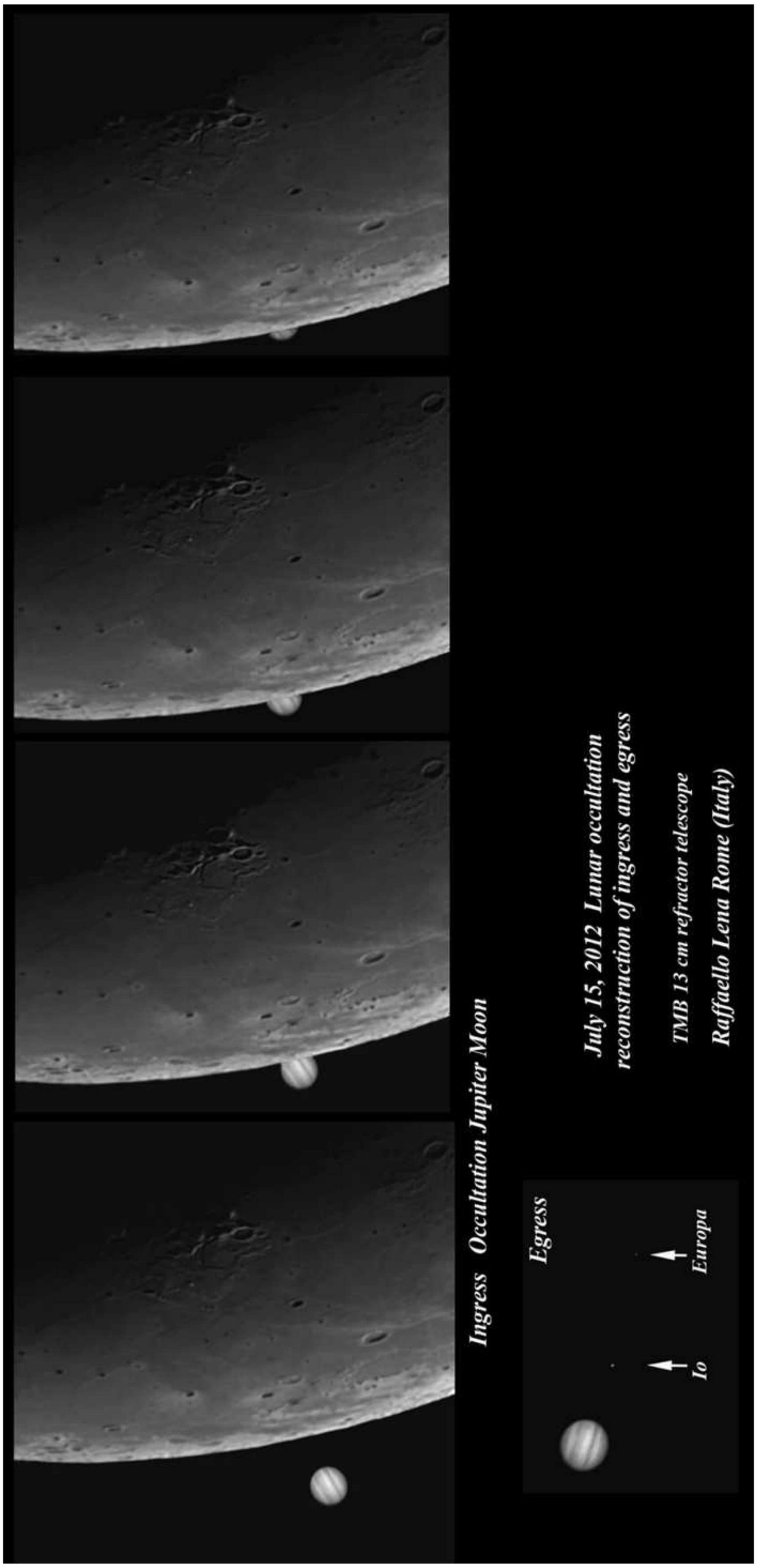

The lunar occultation of Jupiter occurred on July 15, 2012 and it was rare event. A series of images taken with a TMB 13 cm refractor, showing the ingress phase of the planet in the reconstruction of the occultation, are presented. Moreover an image of the egress was taken, despite the difficult occultation

Selenology Today

Richard Hill (USA)

Daytime Venus occultation by the Moon.

GLR GROUP.org
Geological Lunar Researches Group